Journal of Hazardous Materials 507 (2026) 141770

Contents lists available at ScienceDirect

Journal of Hazardous Materials

journal homepage: www.elsevier.com/locate/jhazmat

Bioethanol fireplaces as indoor pollution sources: The role of burner design and fuel type

Estela D. Vicente [a,*], Yago Cipoli [a], Isabella Charres [a], Teresa Nunes [a], Mário Cerqueira [a], Manuel Feliciano [b], Nuria Galindo [c], Eduardo Yubero [c], Célia Alves [a], Jiří Ryšavý [d]

[a] Department of Environment and Planning, Centre for Environmental and Marine Studies, University of Aveiro, Aveiro 3810-193, Portugal
[b] CIMO, LA SusTEC, Instituto Politécnico de Bragança, Campus de Santa Apolónia, Bragança 5300-253, Portugal
[c] Atmospheric Pollution Laboratory (LCA), Department of Applied Physics, Miguel Hernandez University, Avenida de la Universidad S/N, Elche 03202, Spain
[d] VSB - Technical University of Ostrava, Energy Research Centre, Ostrava-Poruba 708 00, Czech Republic

HIGHLIGHTS

- Bioethanol fireplaces markedly increased indoor air pollutant levels
- Formaldehyde and NO_2 often exceeded WHO short-term exposure limits
- Burner design and fuel type showed distinct effects on different indoor pollutants
- Increasing fuel load raised most pollutants and PM components but reduced VOC levels
- PM_{10} generated during combustion showed high oxidative potential

GRAPHICAL ABSTRACT

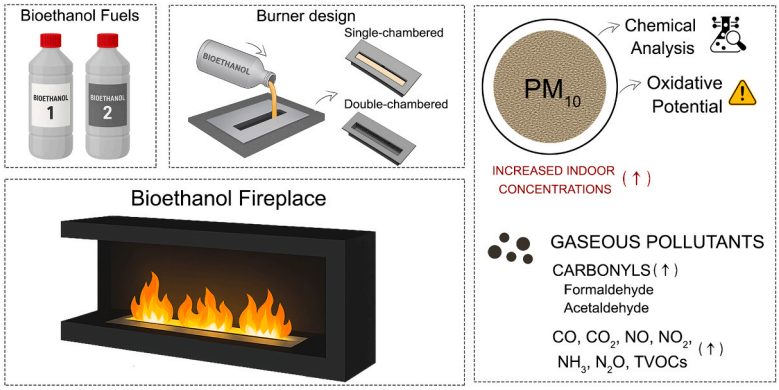

ARTICLE INFO

Keywords:
Inorganic gases
VOCs
Carbonyl compounds
Oxidative potential
PM-bound species

ABSTRACT

Bioethanol fireplaces are marketed as clean and decorative heating alternatives. However, their impact on indoor air quality (IAQ) remains poorly characterised. This study investigates the indoor levels of gaseous and particulate pollutants using a bioethanol fireplace operated under realistic conditions. Two types of bioethanol fuels and two burner designs, a single-chambered (SC) and a double-chambered (DC), were tested under minimal ventilation. Concentrations of CO, NO, NO_2, CO_2, NH_3, N_2O, C_2H_6O, total volatile organic compounds (TVOCs), and carbonyl compounds were measured, while particulate matter (PM_{10}) was characterised chemically and toxicologically. Combustion of both fuels led to substantial increases in indoor pollutant concentrations compared to background levels. Indoors, maximum average CO levels reached 5.67 μg m^{-3}, NO 0.33 μg m^{-3}, NO_2 0.85 μg m^{-3} and TVOCs exceeded 1400 μg m^{-3}. Acetaldehyde and formaldehyde were the dominant carbonyls, with the latter frequently surpassing the WHO guideline value along with NO_2. Compared with traditional wood combustion, bioethanol combustion produced relatively higher indoor concentrations of nitrogen oxides, acetaldehyde, and formaldehyde. Average PM_{10} concentrations ranged from 31.5 to 173 μg m^{-3}, with

* Corresponding author.
E-mail address: estelaavicente@ua.pt (E.D. Vicente).

https://doi.org/10.1016/j.jhazmat.2026.141770
Received 3 December 2025; Received in revised form 11 March 2026; Accepted 12 March 2026
Available online 13 March 2026

higher indoor concentrations for the DC burner and Fuel 2. PM_{10} samples were enriched in bromine, ammonium and nitrate during combustion, and exhibited elevated oxidative potential. Differences in indoor pollutant levels and oxidative potential were observed depending on the burner design, fuel type and initial fuel load. These results demonstrate that flueless bioethanol fireplaces can markedly deteriorate IAQ, underscoring the need for performance standards, improved fuel formulations, and adequate ventilation to mitigate exposure risks associated with their use.

1. Introduction

Air pollution is consistently identified as a major global determinant of premature mortality [1]. In Europe, regulatory measures have substantially reduced ambient pollutant concentrations over recent decades. Nevertheless, these improvements do not account for exposures occurring indoors. Enclosed environments, where people spend nearly nine-tenths of their daily lives [2,3], frequently exhibit high pollutant levels, making indoor air quality (IAQ) a major determinant of comfort, productivity, and health [4–6]. Despite its long-standing relevance, IAQ only became the focus of systematic scientific research in the 1970s, when concerns over energy conservation, emerging health problems, and new measurement technologies highlighted the need to better understand indoor exposures [7]. Research on indoor air pollution has expanded rapidly over the past decade, reflecting increasing recognition of its contribution to the global burden of disease [7,8]. Nevertheless, compared with outdoor air, indoor environments remain relatively understudied. Recent work has highlighted this imbalance, calling for systematic, standardised, and long-term approaches to measuring indoor air chemistry across diverse building types and climates, and emphasising that IAQ is not simply a reflection of outdoor pollution infiltration but the outcome of interconnected physical, chemical, and social processes that remain insufficiently addressed in current regulatory frameworks [9]. Recent reviews emphasise that indoor air pollution results from complex interactions between indoor and outdoor sources, including building materials, combustion processes, occupant activities, and ventilation dynamics [8,10,11]. These pollutants include inorganic gases (e.g., SO_2, NOx, CO_2, CO, radon), volatile organic compounds (VOCs), particulate matter (PM), combustion by-products (BC, PAHs), and biological agents (fungi, bacteria, allergens), all associated with adverse respiratory, cardiovascular, and neurological effects [4,8,12,13].

Among residential pollution sources, major contributors include smoking, cleaning, cooking, and solid fuel combustion [14–21]. Residential heating, in particular, plays a significant role in indoor air pollution. While the impacts of solid fuel combustion are relatively well documented [19,22–27], the effects of emerging heating technologies on IAQ remain largely understudied. Among these emerging alternatives, (bio)ethanol fireplaces have gained significant popularity in Europe [28]. Marketed primarily as decorative or supplementary heating devices, they attract consumers through a blend of modern design and the perception of being environmentally friendly [29]. The combustion of hydrocarbon fuels such as ethanol ideally oxidises carbon and hydrogen to carbon dioxide and water, but real-world conditions rarely achieve this efficiency. The quality of the combustion process depends not only on the amount of air supplied but also on how effectively it mixes with the flame: air introduced within or immediately downstream of the flame promotes oxidation, while excess air added later mainly dilutes exhaust gases without lowering pollutant loads. In flueless appliances like ethanol fireplaces, where all combustion by-products are released indoors rather than vented outside, the accumulation of pollutants poses a direct risk to air quality [28]. Fuel quality further influences performance, as denatured ethanol varies in water content, additives, and denaturants that affect heating value, efficiency, and emissions [29–31]. Thus, incomplete combustion, driven by factors such as burner design, fuel purity, and air excess ratio, often produces harmful by-products in addition to theoretically expected CO_2 and water [28].

Despite their growing market share, only a limited number of studies have investigated the IAQ impacts of bioethanol fireplaces, most of them conducted under controlled chamber conditions. These studies have examined a range of pollutants, including CO, CO_2, NOx, aldehydes, VOCs, PM, and odours [29,32–34]. Results indicate that concentrations of certain pollutants, such as NO_2, and formaldehyde, can approach or exceed guideline values.

Among indoor pollutants, PM is of particular concern due to its established links with respiratory, cardiovascular, and neurological diseases [35]. Despite these risks, epidemiological assessments of indoor-generated particles remain limited and exposure control strategies underdeveloped. Indoor particle events are short-lived yet can reach concentrations far above background levels, often dominating personal exposure. Ultrafine particles may account for 19–76% of exposure depending on activity and conditions, with up to 30% of the global PM-related disease burden potentially linked to indoor emissions [36]. Ethanol combustion in fireplaces has been shown to release PM, however, its chemical composition is poorly characterised, and little is known about its toxicity. In particular, data on oxidative potential (OP), a key indicator of PM toxicity and an important metric for assessing health risks [37–40], are lacking.

Given the increasing popularity of (bio)ethanol fireplaces, further research is urgently needed to better assess exposure risks and guide safe consumer use. In this context, the present study provides a comprehensive assessment of IAQ during the operation of a decorative bioethanol fireplace, combining gas-phase measurements with PM_{10} chemical characterisation and OP assessment. IAQ was assessed for different burner-fuel combinations simulating real-world operation. Understanding these dynamics is critical to inform guidelines and recommendations for the safe use of bioethanol fireplaces.

2. Methodology

2.1. Study design

The measurements were conducted in a 74.34 m^3 room located at the University of Aveiro. The bioethanol fireplace (400 ×1200 x 165 mm) used was a wall-mounted model with three burners (3 ×1 kW). To simplify installation, additional legs were designed and attached to allow the fireplace to stand freely. These legs were constructed as part of the outer structure, ensuring they did not interfere with the combustion process. The fireplace was positioned against a wall to replicate typical usage conditions.

Indoors, all measurement devices were placed in the centre of the room at a height of 1.5 m above the floor to represent the breathing zone of occupants (Fig. 1). To evaluate the effect of different burner types on IAQ, two burner designs were tested: single-chambered (SC) burner and double-chambered (DC) burner. The detailed description of the burners can be found in a previous study [41]. Briefly, SC burners had a single chamber filled with ceramic wool, whereas DC burners were divided into two chambers. The first chamber, used for fuel dosing, while the second chamber was filled with ceramic wool. Fuel is introduced into the first chamber, where it forms a layer and gradually saturates the ceramic wool in the second chamber across its full width. Each configuration was equipped with three burners to simulate a typical setup for the fireplace. All three burners were operated simultaneously with the

same amount of initial fuel dose. For each burner design, two different brands of commercial bioethanol fuels were tested (Table 1). Auto-ignition temperatures were determined following EN ISO/IEC 80079–20–1 using the AIT 551 apparatus (OZM). Higher heating values (HHVs) were measured using a LECO AC600 calorimeter and lower heating values (LHVs) were recalculated according to DIN 51900–1. Water content was quantified using a Mettler Toledo T5 titrator. More details can be found elsewhere [30]. The elemental composition of the fuels (Table 1) and ceramic wool (Table S1) was determined semi-quantitatively by X-ray fluorescence using a Spectro XEPOS energy dispersive spectrometer (Spectro, Germany). Samples were placed in a plastic cuvette with a Mylar protective foil and then analysed in a protective atmosphere (He).

The measurement protocol was designed to evaluate indoor pollutant concentrations under minimum ventilation conditions, which are typical during cold weather when doors and windows remain closed.

Before the combustion tests, baseline pollutant levels were monitored to assess the impact of the bioethanol fireplace on IAQ. For each combustion experiment, the bioethanol fireplace was ignited with the burners fully open and the fuel reservoirs filled to near its maximum capacity (200 mL) to replicate typical usage conditions. A graduated cylinder was used to ensure the accurate addition of fuel to each burner. Additionally, a set of tests to evaluate the fuel load was conducted using Fuel 1 (250 mL) and DC burners (hereafter referred to as DC*). The duration of each combustion experiment, the amount of fuel burned during each test, as well as other relevant experimental details, are provided in Table 2. The combustion tests were concluded when the flames from all three burners were extinguished. Each combustion experiment was repeated four times, in distinct days. A total of 20 combustion experiments were conducted. Carbonyl measurements were performed on three of the four sampling days. The combustion duration generally ranged from 59 min to about 1 h and 20 min, depending on the burner and fuel load. The air exchange rate (AER) was determined using the CO_2 decay method, following the approach described by Vicente et al. [42].

Table 1
Characteristics of the fuels tested.

	Fuel 1	Fuel 2
HHV(MJ·kg^{-1})	27.8	29.4
LHV (MJ·kg^{-1})	25.1	26.6
w_{water}	0.054	0.005
Autoignition temperature (°C)	401 ± 3	397 ± 3
mg kg^{-1}		
Mg	bdl	171
Si	71.7	129
P	996	885
Ca	494	424
Ti	2.0	2.70
V	0.8	0.40
Cr	1.2	1.10
Mn	2.1	2.50
Fe	18.3	15.3
Ni	2.2	1.90
Cu	1.2	1.40
Zn	1.5	1.50
Rb	0.2	0.20
Sr	0.2	0.30
Y	0.6	0.40
Zr	0.7	0.40
Nb	0.7	bdl
Cd	2.6	2.10
I	bdl	5.80
Ba	20.1	bdl
Ce	40.7	71.0
Hf	3.2	1.10
Ta	23.3	16.8
Th	0.4	0.40
U	0.8	0.80

Several elements were below the detection limit (bdl). Limit of Detection (mg kg^{-1}): Mg (101), S (2.0), Cl (2.0), K (10), Al (20), Co (3.0), Ga (0.5), Ge (0.5), As (0.5), Se (0.5), Br (0.5), Nb (0.3), I (3.5), Ba (2.0), Mo (1.0), Ag (2.0), Sn (3.0), Sb (3.0), Te (3.0), Cs (4.0), La (2.0), W (0.5–0.4), Hg (1.0), Tl (1.0), Pb (0.2–0.1), Bi (1.0).

2.2. Monitoring of gaseous compounds

Concentrations of CO, NO_2, and NO were measured at 5-min intervals throughout the baseline, combustion, and post-combustion phases using Horiba analysers (APMA-370, APNA-370). Additional measurements of N_2O, CO_2, NH_3, and C_2H_6O were obtained with a multi-gas analyser (Gasera ONE, Gasera). Total VOCs (TVOCs) were monitored with a Wolfsense IQ-610 probe (Gray Wolf®). Prior to the sampling campaign, the analysers were calibrated with gas calibration bottles containing known gas concentrations.

For the collection of carbonyl compounds, commercial cartridges containing silica gel, as the solid adsorbent, coated with 2,4-dinitrophenylhydrazine (DNPH) (Sep Pack, Waters) were used. The sampling system comprised a DNPH cartridge, a needle valve, a vacuum pump, and a dry gas meter. The dry gas meter was calibrated using a wet gas meter, and the sampled volume was corrected using the obtained calibration

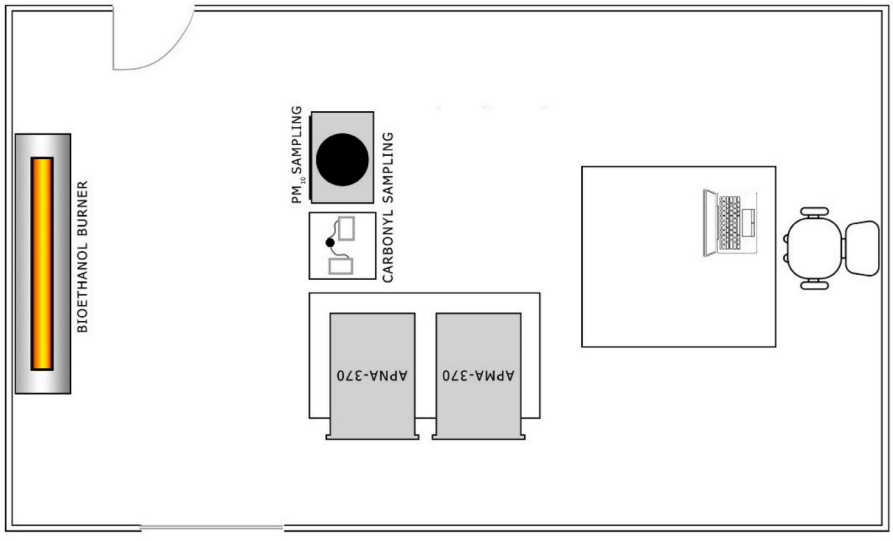

Fig. 1. Layout of the indoor experimental setup.

Table 2
Description of the experiments conducted.

Test	Fuel	Burner	Fuel load for each burner (mL)	Regulation flap (%)	Carbonyl sampling	Duration (hh:min)	Air exchange rate (h^{-1})
#1	Fuel 1	DC*	250	100	✓	1:20	0.48
#2	Fuel 1	DC*	250	100	✓	1:19	0.36
#3	Fuel 1	DC*	250	100	✓	1:18	0.46
#4	Fuel 1	DC*	250	100	⊗	1:19	0.41
#1	Fuel 1	SC	200	100	✓	1:04	0.53
#2	Fuel 1	SC	200	100	✓	1:05	0.43
#3	Fuel 1	SC	200	100	✓	1:05	0.60
#4	Fuel 1	SC	200	100	⊗	1:05	0.32
#1	Fuel 1	DC	200	100	✓	1:12	0.56
#2	Fuel 1	DC	200	100	✓	1:12	0.47
#3	Fuel 1	DC	200	100	✓	1:15	0.45
#4	Fuel 1	DC	200	100	⊗	1:13	0.50
#1	Fuel 2	DC	200	100	✓	1:03	0.55
#2	Fuel 2	DC	200	100	✓	1:04	0.39
#3	Fuel 2	DC	200	100	✓	1:03	0.49
#4	Fuel 2	DC	200	100	⊗	1:03	0.61
#1	Fuel 2	SC	200	100	✓	1:04	0.62
#2	Fuel 2	SC	200	100	✓	1:03	0.37
#3	Fuel 2	SC	200	100	✓	0:59	0.48
#4	Fuel 2	SC	200	100	⊗	1:00	0.32

factor. Three replicate samples were collected on different days for each condition indoors. The sampling strategy included a 1-hour sample prior to the combustion experiment and one sample collected during the combustion period. Outdoors, one sample per week was collected. The sampling flow was 2 L min^{-1}.

The carbonyl compounds, in the form of hydrazones, were eluted in the reverse direction of loading from the cartridges with 3 mL of acetonitrile and analysed using a reverse-phase high-performance liquid chromatography system with a diode array (Shimadzu Prominence, Germany). The HPLC consists of a degasser (model DGU-20ASR), a solvent distributor (model LC-30AD), an automatic sampler (model SIL-30AC), a diode array detector (model SPD-M20A), and an oven (model CTO-20AC) containing an Ascentis C18 SUPELCO column (15 cm×4.6 mm, 5 μm). The Lab Solutions software was used to carry out data processing and system control. A ternary elution gradient (water, acetonitrile, and tetrahydrofuran) was used for the analysis. The gradient analysis begins with a mixture composed of 70% mobile phase A (20% acetonitrile, 60% MilliQ water, and 20% tetrahydrofuran) and 30% mobile phase B (60% acetonitrile and 40% MilliQ water). After 30 min, the gradient is adjusted to 100% mobile phase B and maintained under this condition for 30 min. At 85 min, the gradient returns to the initial condition (70% A and 30% B), marking the end of the analysis. The flow rate was set at 0.6 mL min^{-1} throughout the analysis. The injection volume was 10 μL and the column temperature was maintained at 22°C. Quantification was performed using a commercial standard solution containing various carbonyl compounds in the form of hydrazones (TO11/1P6A carbonyl-DNPH mix).

2.3. PM sampling

For PM_{10} sampling, high-volume samplers (MCV, model CAV-A/mb) operating at a constant flow rate of 30 m^3 h^{-1} were used indoors and outdoors during the burning period. Particulate matter was collected on 150 mm quartz fibre filters (Pallflex®) and weighed on a microbalance before and after sampling. Background measurements, collected over a 24-h period with the source inactive, and field blanks were included in the analysis. Indoors, the sampling inlet was centrally placed at 1.5 m height, while outdoors, it was placed at a similar height on a patio adjacent to the room where the experiments were conducted.

Indoors, continuous PM_{10} monitoring employed a light-scattering laser photometer (DustTrak DRX 8533, TSI Inc., Shoreview, MN, USA). The equipment underwent manufacturer calibration before the campaign, operated at 1-min resolution, and pre-measurement checks (zero, inlet cleaning) were conducted. Photometric devices offer high spatiotemporal resolution but can exhibit deviations due to aerosol properties.

2.3.1. PM_{10} chemical analysis

Water-soluble organic carbon (WSOC) was extracted from pieces of PM_{10} filters by ultrasonic agitation in ultrapure water and quantified using a Shimadzu TOC-L CSH analyser based on catalytic oxidation at 680 °C. Samples were diluted 1:2, acidified with 1 M HCl, purged with ultrapure air, and analysed in triplicate. Calibration used potassium hydrogen phthalate, and procedural blanks were included for quality control [43].

Elemental composition was determined by energy-dispersive X-ray fluorescence (ED-XRF) using an ARL Quant'X spectrometer (Thermo Fisher). Samples were excited with a Rh-anode X-ray tube under vacuum, using multiple filter/voltage settings to optimise sensitivity. Calibration was done with Micromatter standards and verified with NIST SRM2783. Spectral analysis was performed using the WinTrace software [44].

For the quantification of water-soluble ions, two 19 mm punches from each filter sample were extracted with 5 mL of ultrapure Milli-Q water using ultrasonic agitation (15 + 15 min). The extracts were then filtered through a 13 mm PVDF syringe filter with a 0.2 μm pore size (Whatman™). Anions were determined using an ICS-3000 SP pump (Dionex, USA) coupled with a Gilson 234 injector, a Dionex AS14 analytical column and AG14 guard column (4 × 250 mm), a Dionex AMMS-300 suppressor, and a CTO-6A column oven (Shimadzu) equipped with a conductivity cell connected to a Shimadzu CDD-6A detector. The regenerant was 50 mM H_2SO_4, and the eluent consisted of a mixed solution of 2.2 mM Na_2CO_3 and 2.8 mM $NaHCO_3$, both delivered at a flow rate of 2.0 mL min^{-1}. Cations were analysed using a Thermo Fisher Scientific Dionex Aquion ion chromatograph equipped with an AS-AP autosampler maintained at 20 °C, a quaternary pump with a 10 μL sample loop, a DS6 heated conductivity cell, and an eluent regenerator system (Dionex CDRS 600, 2 mm). Separation was achieved with a Dionex IonPac CS16 analytical column (3 × 250 mm) maintained at 30 °C, preceded by a CG16 guard column (3 × 50 mm). The eluent was 20 mM methanesulfonic acid (MSA), delivered at 0.36 mL min^{-1}. Instrumental control, data acquisition, and chromatographic integration were carried out using the Dionex Chromeleon™ software. Calibration was performed at the beginning of each analytical sequence using standard solutions prepared from high-purity reagents (Sigma-Aldrich). Quantification was based on external calibration curves generated for each ion species.

2.3.2. PM_{10} oxidative potential analysis

A portion from each PM_{10} quartz sample was extracted in 12 mL of Milli-Q water using ultrasonic agitation (30 min). The extracts were filtered through 0.2 μm PVDF syringe filters and analysed immediately. The ascorbic acid (AA) and dithiothreitol (DTT) assays were performed following the method of Gómez-Sánchez et al. [43]. Briefly, for the AA assay, 1.5 mL of extract was mixed with 1.35 mL of 0.1 M potassium phosphate buffer (pH 7.4) and 150 μL of 2 mM AA and then incubated at 37 °C. Absorbance at 265 nm was recorded at 15, 30, and 45 min to track AA depletion. In the DTT assay, three 0.45 mL aliquots of extract were incubated with 90 μL buffer and 60 μL of 1 mM DTT at 37 °C. After 15, 30, and 45 min, reactions were stopped with 0.5 mL of 10% trichloroacetic acid. Samples then reacted with 2 mL of Tris-EDTA buffer and 50 μL of 10 mM DTNB, and absorbance was measured at 412 nm.

Filter blanks were run in parallel, and blank depletion was subtracted. All analyses were performed in duplicate. OP values (OP^{AA} and OP^{DTT}) were expressed in nmol min^{-1} m^{-3} and pmol min^{-1} μg^{-1}.

3. Results

3.1. Gaseous pollutants

Several gaseous species were monitored indoors during the combustion experiments and under background conditions (in the absence of the combustion source). The average concentrations are presented in Table 3, and the temporal profiles for each species are shown in Figure S1. Background concentrations were consistently low. Following ignition of the ethanol-based fuels, the concentrations of several combustion by-products increased sharply. For most species, a single peak was observed toward the end of the combustion period (Figure S1A-F). In contrast, TVOCs and C_2H_6O exhibited two distinct peaks, one immediately after ignition and another at the end of combustion (Figure S1G and S1H).

Regarding CO, clear differences in average indoor concentrations between burner designs and fuel types were recorded. The DC burner operating with Fuel 1 produced the highest CO concentrations, averaging 5.67 mg m^{-3} at a 200 mL fuel load and 5.40 mg m^{-3} at a 250 mL load. With Fuel 2, the average CO levels decreased to 4.01 mg m^{-3} for the DC design and to 2.66 mg m^{-3} for the SC design. For both fuels, the SC burner consistently produced lower average CO levels than the DC burner. When compared to background levels (0.18 ± 0.02 mg m^{-3}), all burner designs resulted in several-fold increases in emissions. The magnitude of the increase was particularly pronounced for the DC burner, for which concentrations were more than twenty times higher than baseline. Nevertheless, the WHO short-term exposure guideline of 35 mg m^{-3} for CO (1-h averaging time) was not exceeded in any of the tested scenarios. These findings are consistent with the concentrations previously reported by Guillaume et al. [29] and Schripp et al. [34]. The average indoor CO concentrations measured during bioethanol fireplace operation were within the range reported for traditional wood-burning heating appliances. However, indoor CO concentrations associated with wood combustion vary widely, from 0.78 to 7.1 mg m^{-3} in multiple studies [45–47] up to 45.8 mg m^{-3} [48].

The elevated CO levels observed for the DC design can be attributed to its internal geometry. The DC burner introduces a partition that disrupts the uniform flow of fuel vapours, potentially creating regions of incomplete mixing and localised oxygen deficit. Such conditions are conducive to incomplete combustion, which is reflected in the higher CO emissions measured for this burner type. This outcome aligns with fluid dynamics principles, where internal barriers reduce turbulence and delay air-fuel mixing in low-pressure diffusion combustion environments [30]. Regarding the effect of fuel composition, Ryšavý et al. [49] reported that CO emissions were lowest during combustion of pure ethanol and increased markedly with the addition of water. This behaviour was attributed to the cooling effect associated with water evaporation, which lowers flame temperature and promotes incomplete oxidation, thereby increasing CO formation. This mechanism is consistent with the higher CO emissions observed Fuel 1 in the present study.

CO_2 concentrations during combustion were substantially elevated compared to background levels (average of 925 mg m^{-3}), ranging from 2914 to 3522 mg m^{-3} across burner-fuel combinations. The highest average CO_2 level (3522 mg m^{-3}) was recorded for Fuel 1 in the DC* design (initial load 250 mL), while the lowest occurred for Fuel 2 DC (2914 mg m^{-3}). It should also be noted that measured CO_2 concentrations were affected by the presence of two individuals in the room during testing, as human respiration is a continuous source of CO_2. During background measurements the room was empty. The CO_2 concentrations measured in the present study are lower than those reported by Guillaume et al. [29] and Schripp et al. [34], which may be attributed to several factors, including room volume, air exchange rates, and fuel load.

NO and NO_2 were detected during the operation of both burner designs. The SC burner consistently produced higher NO (0.29 and 0.33 mg m^{-3} for Fuel 1 and 2, respectively) indoor concentrations than the DC system (0.12 and 0.16 mg m^{-3} for Fuel 1 and 2, respectively). This observation can be attributed to the SC design, where relatively higher flame temperatures and shorter quenching distances can enhance NO generation via the thermal mechanism [30]. In contrast, NO_2 concentrations varied less between burner designs, with the highest average concentrations recorded for the DC burner design (Fuel 1). During fireplace operation, indoor NO_2 concentrations surpassed the WHO short-term (1-h, 0.200 mg m^{-3}) exposure guideline across all burner and fuel combinations. Nitrogen oxide formation in ethanol flames proceeds mainly through the thermal mechanism, with the prompt pathway having a minor contribution due to the low CH radical concentrations in alcohol flames. Thus, it was observed that NO dominates over NO_2 in the flame zone itself [50]. The comparatively higher average NO_2 concentrations observed in the present study might be attributed to post-flame oxidation of NO to NO_2 promoted by the high oxygen availability. The effects of fuel type and initial load on indoor NO and NO_2 levels were less pronounced than those of burner design. Fuel 2 produced slightly higher concentrations of NO, which may be related to its lower water content. As reported previously, water in the fuel can lower flame temperatures and thereby suppress thermal NOx formation [49]. The amount of fuel loaded into the burner also influenced emissions. Higher fuel loads (250 mL, Fuel 1), resulted in slightly elevated

Table 3
Average concentrations of gaseous species measured indoors during and in the absence of combustion (background).

	Fuel 1 DC*	Fuel 1 DC	Fuel 1 SC	Fuel 2 DC	Fuel 2 SC	Background
CO (mg m^{-3})	5.40 ± 2.40	5.67 ± 2.55	3.13 ± 1.63	4.01 ± 2.70	2.66 ± 1.52	0.18 ± 0.02
CO_2 (mg m^{-3})	3522 ± 955	3403 ± 838	3376 ± 957	2914 ± 1241	3362 ± 953	925 ± 55.8
NO (mg m^{-3})	0.22 ± 0.15	0.12 ± 0.09	0.29 ± 0.21	0.16 ± 0.17	0.33 ± 0.26	(1.0 ± 0. 4) × 10^{-3}
NO_2 (mg m^{-3})	0.85 ± 0.43	0.79 ± 0.39	0.66 ± 0.34	0.64 ± 0.51	0.64 ± 0.39	(1.0 ± 0.2) × 10^{-2}
NH_3 (mg m^{-3})	1.55 ± 0.39	1.55 ± 0.38	1.48 ± 0.40	1.24 ± 0.45	1.41 ± 0.38	0.54 ± 0.19
N_2O (mg m^{-3})	5.49 ± 2.14	5.07 ± 1.82	4.95 ± 2.07	4.17 ± 2.52	4.95 ± 2.09	0.77 ± 0.07
C_2H_6O (mg m^{-3})	18.7 ± 5.33	26.7 ± 6.25	18.1 ± 4.76	18.2 ± 7.76	17.9 ± 4.22	2.09 ± 0.70
TVOC (μg m^{-3})	1069 ± 319	1410 ± 341	1001 ± 265	1484 ± 685	1102 ± 294	230 ± 56

NO and NO_2 concentrations. This suggests that increasing fuel quantity alters combustion dynamics in a way that promotes higher flame temperatures and, consequently, greater thermal NOx generation. Relative to background levels, indoor NO concentrations increased by approximately 120- to 330-fold, while NO_2 concentrations increased by about 64- to 85-fold. These results contrast with those reported by Salthammer et al. [45] from indoor measurements in private households, where operation of wood-burning appliances was reported to have only a marginal or no influence on indoor NO and NO_2 concentrations. Similarly, Lévesque et al. [51] reported that indoor NO_2 concentrations were not significantly influenced by the presence of wood combustion appliances in Canadian homes.

Other nitrogen-containing species were also found to increase during the combustion experiments. Ammonia (NH_3) concentrations rose consistently to values ranging from 1.24 to 1.55 mg m^{-3} compared to background levels of 0.54 mg m^{-3}, while nitrous oxide (N_2O) increased from an average of 0.77 mg m^{-3} in background air to 4.17 – 5.49 mg m^{-3} depending on the fuel and burner type. The most likely explanation is that, after the initial NOx pool is formed through the thermal mechanism, the radical-rich and partially reducing environment created by incomplete ethanol combustion (with CO, H_2, and hydrocarbon fragments present) enables further nitrogen chemistry. Such conditions favour pathways in which NOx can be reduced to NH_3 and stabilised as N_2O. For instance, NH_2 radicals formed in the flame can react with HNO or HONO to regenerate NH_3. At the same time, reactions of amine radicals with NOx provide efficient channels for N_2O formation [52].

Indoor TVOC concentrations increased from 230 μg m^{-3} under background conditions to 1001–1484 μg m^{-3} during bioethanol combustion, depending on fuel type and burner design. Among the tested fuels, Fuel 2 produced the highest concentrations. This may be attributed to its lower water content and higher heating value, which can lead to higher operating temperatures [49] and, consequently, enhanced fuel evaporation [33]. Additionally, the DC burner generated consistently higher concentrations than the SC burner. The fuel load also influenced the average TVOC levels. Higher fuel loads (250 mL, Fuel 1) resulted in lower TVOC concentrations. Schripp et al. [34] identified ethanol and the denaturant 2-butanone as dominant VOCs during combustion, with gel fuels also releasing 2-propanol. Additionally, their chamber experiments detected formaldehyde and benzene at concentrations exceeding health-based guideline values. Complementary results from Nozza et al. [33] further demonstrated that VOC and odour emissions from bioethanol fireplaces are strongly influenced by burner design and ventilation. They observed that VOC concentrations remained relatively low during operation but increased sharply during the shutdown phase due to evaporation of residual hot fuel. Ethanol was again the dominant compound, accompanied by heavier alcohols (e.g., 2-propanol), oxygenated organics, and aromatics such as toluene. Odour emissions correlated with increased VOC release from open-tank or porous burner designs. In the present study, ethanol indoor concentrations also rose significantly compared to background levels (2.09 mg m^{-3}) regardless the fuel and burner design tested. The highest increase was observed for Fuel 1 combustion using the DC burner (26.7 mg m^{-3}). Although this represents a substantial rise relative to baseline conditions, it remains well below the Occupational Safety and Health Administration (OSHA) permissible exposure limit for ethanol of 1900 mg m^{-3} (8-h time-weighted average).

Table 4 summarises the concentrations of carbonyl compounds measured before and during combustion under the various test conditions, as well as the outdoor levels. In all cases, formaldehyde and acetaldehyde levels increased substantially during fireplace operation compared with the pre-combustion phase, confirming their consistent formation as primary combustion by-products. Formaldehyde concentrations rose between 5- and 14-fold, with increases from 10.5 to 21.0 μg m^{-3} (before) to 90.8 – 179 μg m^{-3} (during). Acetaldehyde showed even more pronounced increases, rising between 24- and 72-fold, from 4.27 to 8.06 μg m^{-3} before combustion to 174–411 μg m^{-3} during fireplace operation. These results confirm that both compounds are dominant by-products of ethanol combustion. Propionaldehyde also showed an increase, although to a lesser extent. Other carbonyl species, including acrolein, crotonaldehyde, isovaleraldehyde, m-, p-, and o-tolualdehyde, and 2,5-dimethylbenzaldehyde, were either not detected or present at similar concentrations before and during combustion, irrespective of fuel type or burner design. These results align with previous studies that identified formaldehyde and acetaldehyde as the dominant carbonyl emissions from ethanol fireplaces [32,34]. Outdoor concentrations of the detected compounds were lower than those measured indoors under background conditions.

Consistent with previous findings, acetaldehyde was the most abundant compound detected, regardless of fuel type or burner design [29,32]. The formation of acetaldehyde during ethanol oxidation primarily involves hydrogen abstraction by OH and other radicals. Abstraction at the α-carbon yields the α-hydroxyethyl radical ($CH_3\dot{C}HOH$), which rapidly oxidises to acetaldehyde, while abstraction at the hydroxyl group produces the ethoxy radical ($CH_3CH_2O\cdot$), another direct precursor. At elevated temperatures, β-scission of $C_2H_5O\cdot$ radicals

Table 4
Average carbonyl concentrations (μg m^{-3}) measured indoors and outdoors before and during the operation of the bioethanol fireplace under various conditions. Isovaleraldehyde, m-, p-, and o-tolualdehyde, and 2,5-dimethylbenzaldehyde were never detected.

	Fuel 1, DC*		Fuel 1, DC		Fuel 1, SC		Fuel 2, DC		Fuel 2, SC		Outdoor
Compound	Before	During	Before	During	Before	During	Before	During	Before	During	
Formaldehyde	10.5 ± 3.46	152 ± 3.23	18.5 ± 1.69	179 ± 4.57	17.4 ± 1.57	114 ± 19.17	21.0 ± 3.00	146 ± 7.62	18.4 ± 1.62	90.8 ± 4.89	0.46 ± 0.37
Acetaldehyde	4.27 ± 1.71	308 ± 9.32	7.24 ± 1.07	411 ± 44.4	6.71 ± 1.70	229 ± 45.2	8.06 ± 2.14	303 ± 30.6	7.12 ± 0.99	174 ± 10.2	0.23 ± 0.12
Acrolein	ND	ND	ND	0.50 ± 0.86	ND	ND	ND	ND	ND	ND	ND
Propionaldehyde	1.02 ± 0.19	2.43 ± 0.334	1.24 ± 0.14	2.39 ± 0.25	1.27 ± 0.06	1.66 ± 0.46	1.81 ± 0.30	2.32 ± 0.54	1.08 ± 0.43	1.38 ± 0.43	0.42 ± 0.42
Crotonaldehyde	ND	ND	ND	0.50 ± 0.86	ND	ND	ND	ND	ND	ND	ND
Butyraldehyde	1.25 ± 0.31	ND	1.50 ± 0.10	1.47 ± 0.31	1.61 ± 0.15	1.58 ± 0.12	1.79 ± 0.22	ND	0.60 ± 1.04	0.57 ± 0.57	ND
Benzaldehyde	1.22 ± 0.35	1.66 ± 0.33	1.78 ± 0.22	1.58 ± 0.18	1.95 ± 0.14	1.92 ± 0.43	2.21 ± 0.48	1.98 ± 0.22	1.53 ± 0.18	1.42 ± 0.25	ND
Valeraldehyde	0.68 ± 0.14	0.75 ± 0.07	1.21 ± 0.22	1.11 ± 0.16	0.87 ± 0.02	0.95 ± 0.38	1.86 ± 0.62	0.97 ± 0.36	ND	ND	ND
Hexaldehyde	1.91 ± 0.94	2.48 ± 0.41	1.81 ± 0.24	1.69 ± 0.08	1.55 ± 0.20	1.61 ± 0.29	7.04 ± 2.86	3.85 ± 0.33	ND	ND	ND

ND: not detected

provides additional pathways, making acetaldehyde the dominant early intermediate in ethanol oxidation [53,54].

Formaldehyde is a key intermediate that appears downstream in ethanol combustion, formed primarily via β-scission of ethoxy radicals, with additional contributions from secondary oxidation chemistry. These reactions provide a rapid route to formaldehyde, which is subsequently oxidised to CO and ultimately CO_2. Consequently, formaldehyde and acetaldehyde are often observed concurrently in ethanol flames, reflecting successive steps in the degradation of C_2 oxygenates [54]. The acetaldehyde concentrations measured in the present study (174–411 μg m^{-3}) are within the range reported for ethanol fuel combustion in chamber experiments ranging from 150 to 570 μg m^{-3} [53, and references therein]. In contrast, the aldehyde levels observed during bioethanol fireplace operation were substantially higher than those reported for wood-burning appliances in private households. For formaldehyde, Salthammer et al. [45] reported a maximum indoor concentration of 67 μg m^{-3}, with contributions varying depending on the specific appliance and operating conditions. Similarly, acetaldehyde concentrations measured during ethanol fireplace operation exceeded the values reported by Salthammer et al. [45], who found average indoor concentrations in the range of 12–89 μg m^{-3} across six closed appliances and one open appliance. Additionally, Lévesque et al. [51] reported that indoor formaldehyde levels in Canadian homes were not significantly affected by the presence of wood combustion appliances.

In the present experiments, formaldehyde and acetaldehyde concentrations varied with burner design, fuel type, and fuel load (Table 1). Both compounds were consistently higher when using the DC burner, independent of the bioethanol fuel employed. In addition to burner design, the type of bioethanol fuel had a clear influence on carbonyl compound emissions. Combustion of Fuel 1 consistently produced higher formaldehyde and acetaldehyde concentrations than Fuel 2 across both burner types. The higher concentrations of formaldehyde and acetaldehyde observed during combustion of Fuel 1 can be explained by its higher water content, which reduces flame temperature and suppresses complete oxidation of ethanol. Similar effects of water-containing ethanol fuels on combustion temperature and pollutant formation have been reported for ethanol burners, where increased water content led to lower flue gas temperatures and higher emissions of incomplete combustion products (i.e., CO) [49]. Aldehydes, as intermediate oxidation products of ethanol, are particularly favoured under such conditions.

Fuel load also affected carbonyl compound concentrations. When a larger volume of Fuel 1 (DC*, 250 mL) was burned, formaldehyde and acetaldehyde levels were lower than at the 200 mL load. However, as the higher fuel load was tested under a single burner-fuel configuration, this trend should be interpreted cautiously. Ryšavý et al. [41] reported that increasing the fuel load from 50% to 100% of the burner's capacity led to a 9% increase in maximum and a 17% increase in average heat output, attributed to more stable operation and sustained high thermal power. These results suggest that fuel load is a critical parameter influencing combustion stability and, consequently, the emission of incomplete combustion by-products.

Health-based guideline values for formaldehyde and acetaldehyde have been established by various regulatory agencies. According to Salthammer et al. [53], acetaldehyde concentrations associated with acute effects typically range from 500 to 1500 μg m^{-3}. In the present study, acetaldehyde levels were at the lower end of this range, remaining below 500 μg m^{-3} in all cases. By contrast, formaldehyde concentrations frequently exceeded the WHO short-term exposure guideline of 100 μg m^{-3} (30-min average), which has been set to prevent sensory irritation in the general population. This threshold was surpassed in nearly all experimental scenarios. The only exception occurred with Fuel 2 in the SC burner, for which formaldehyde concentrations (90.8 μg m^{-3}) remained slightly below the WHO limit.

3.2. Particulate matter levels and chemical composition

As reported in chamber studies, ethanol flames are sources of particles due to incomplete combustion. In the flame zone, nucleation of VOCs and radicals forms nanoparticles, which subsequently grow through coagulation and condensation [34]. The temporal analysis of the data reveals that the trend in PM_{10} concentration profiles was similar across test repetitions, although the absolute magnitudes of the peaks varied (Fig. 2). The results underscore the importance of maintenance of burner inner surfaces prior to operation. Regarding the temporal profile, PM levels steadily increased, reaching peak concentrations towards the end of the combustion period, followed by a gradual decline, with the maximum time observed to return to baseline levels being approximately 5–6 h. This marked increase in particle levels at the point of flame extinction was also reported in previous studies. Schripp et al. [34] observed a similar phenomenon, noting that particle sizes grew significantly after the flames of ethanol fireplaces were extinguished, in analogy to the "white smoke" emitted when candles are blown out. The sudden cooling of the combustion zone likely results in incomplete oxidation of organic vapours, which then condense onto residual particles, shifting the distribution toward larger diameters.

Both the burner type and bioethanol fuel choice significantly influence PM_{10} levels during fireplace operation. Results consistently showed that PM_{10} peak and average concentrations were higher when using the DC burner compared to the SC, regardless of the bioethanol fuel used. Variations in burner design likely alter combustion temperature, oxygen availability, and mixing efficiency, thereby influencing the extent of incomplete combustion [34].

Average PM_{10} concentrations varied substantially depending on the combustion process and fuel type (Fig. 3). In all experiments, the DC burner produced higher average particle concentrations than the SC burner. When Fuel 1 was burned, the SC burner yielded average indoor levels of 31.5 μg m^{-3}, whereas the DC burner reached 120 μg m^{-3}. These values correspond to approximately three- and twelve-fold increases above background concentrations, respectively. A comparable trend was observed during the combustion of Fuel 2. The SC burner produced average levels of 82.5 μg m^{-3}, while the DC burner generated 165 μg m^{-3}. Thus, for both fuels, burning with the DC design resulted in two- to four-fold higher particle concentrations relative to the SC burner. Increasing the initial fuel load (Fuel 1, DC*, 250 mL) lead to higher particle levels indoors (173 μg m^{-3}) compared with the 200 mL initial load. Indoor-to-outdoor (I/O) ratios consistently exceeded unity under all combustion scenarios, ranging from 1.1 to 9.7.

Using the WHO 24-h PM_{10} air quality guideline as a reference, while noting that the measurements reflect short-term concentrations rather than 24-h averaged exposures, the results indicate that ethanol combustion in fireplaces, particularly with DC burners, can generate indoor particle levels well above recommended exposure limits. While combustion of Fuel 1 in the SC burner remained below the guideline, all other burning conditions, especially Fuel 1 DC and Fuel 2 DC, produced average concentrations two to four times higher than the 24-h limit. Outdoor levels also frequently exceeded the guideline on several days, whereas indoor background concentrations remained low (9.66 μg m^{-3}).

The PM_{10} concentrations observed during bioethanol fireplace operation in the present study are within the range reported for conventional solid fuel heating appliances. While direct comparisons across studies are subject to differences in ventilation, room volume, and usage patterns, this comparison provides a useful frame of reference for evaluating the relative impact of bioethanol fireplaces on indoor air quality. Open wood-burning fireplaces have been shown to produce highly variable PM_{10} concentrations, typically ranging from about 40–212 μg m^{-3} [48,55], but reaching substantially higher levels, up to 550 μg m^{-3}, under certain operating conditions [19,46]. Woodstoves have been associated with indoor PM_{10} concentrations spanning approximately 29–227 μg m^{-3} [19,55,56]. The operation of pellet

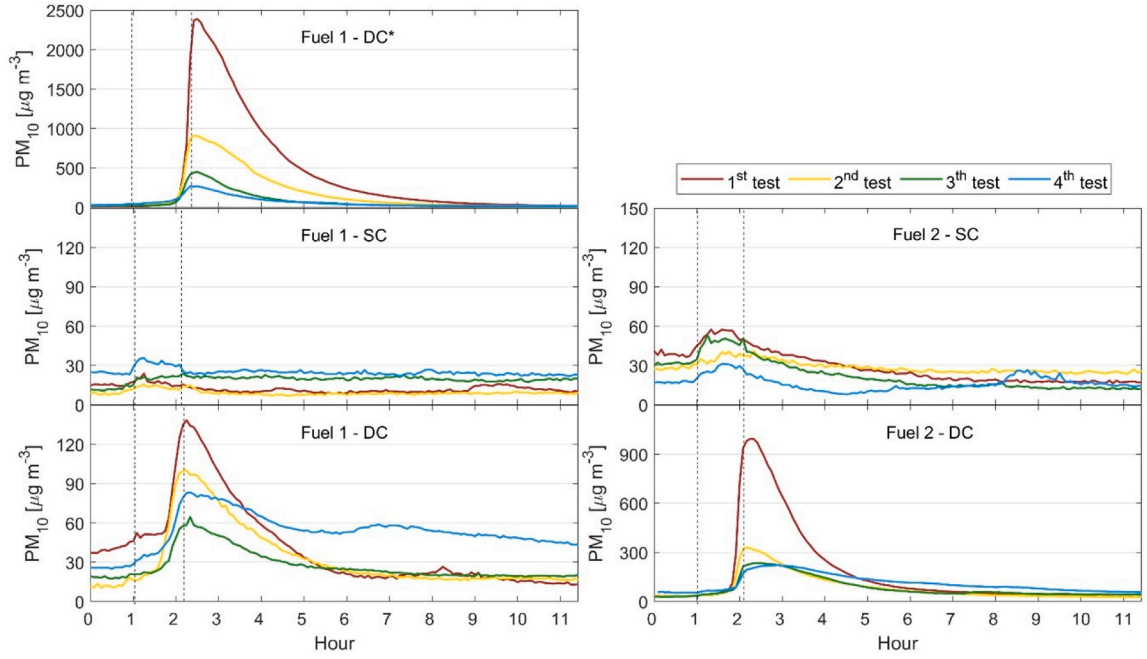

Fig. 2. Indoor PM_{10} concentration profiles (μg m^{-3}) measured before, during, and after the operation of the bioethanol fireplace under various conditions across different sampling days. The combustion period is indicated by a dashed line.

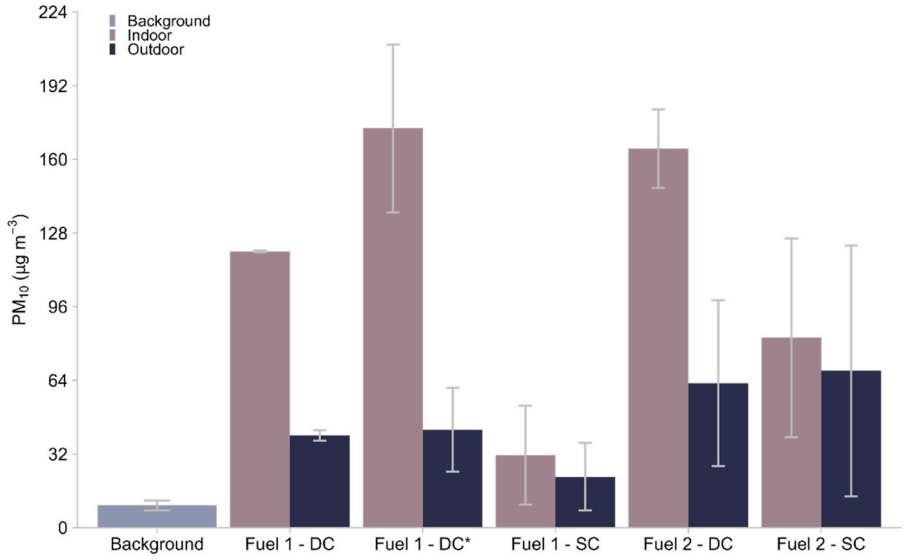

Fig. 3. Average PM_{10} concentrations indoors, during combustion and without indoor activities (background), and outdoors.

stoves generally yield lower indoor PM_{10} concentrations, typically in the range of 16–70 μg m^{-3} [19,56], while coal-fired stoves have been reported to produce PM_{10} levels between 33 and 169 μg m^{-3} [27].

Water-soluble organic carbon (WSOC) represents the oxidised, hydrophilic fraction of organic aerosols that strongly influence indoor air chemistry, secondary formation processes, and human exposure. WSOC contributes to secondary organic aerosol (SOA) formation, affects particle hygroscopicity, and serves as an indicator of oxidative aging and emission sources [57,58]. Moreover, water-soluble aerosol components, including WSOC, are highly bioavailable and strongly correlated with reactive oxygen species generation, linking them to oxidative stress and adverse health effects [58,59]. Given that indoor WSOC concentrations can exceed outdoor levels by an order of magnitude [57], quantifying WSOC is essential for understanding how indoor combustion activities, such as bioethanol fireplaces, affect air quality and human exposure.

The concentrations of WSOC measured during fireplace operation varied across fuels and burner designs (Table 5). The highest indoor WSOC concentrations were recorded for Fuel 1 (4.80 and 5.00 μg m^{-3}, for SC and DC* burner respectively), corresponding to approximately 7 times the indoor background level (0.71 μg m^{-3}). For Fuel 2, indoor average WSOC concentrations ranged from 1.77 to 1.91 μg m^{-3}, representing a 2.5–2.7-fold increase over background, whereas with the DC burner the indoor concentration was slightly lower than outdoors (I/O < 1). Except for Fuel 2 DC, the indoor-to-outdoor ratios (I/O > 1) indicate that the fireplaces acted as an indoor source of water-soluble organic aerosols. The much higher WSOC concentrations observed for Fuel 1 suggest greater emission of oxygenated organic compounds, possibly due to differences in combustion efficiency and fuel formulation. Combustion of Fuel 1 with a 250 mL fuel load (DC*) resulted in the highest average WSOC concentrations. When the fuel load was reduced to

Table 5
Mean and range of PM-bound chemical species indoors (combustion versus background), and outdoors.

	Fuel 1, SC		Fuel 1, DC*		Fuel 1, DC		Fuel 2, DC		Fuel 2, SC		Background	
	Indoor	Outdoor	Indoor	Outdoor	Indoor	Outdoor	Indoor	Outdoor	Indoor	Outdoor	Indoor	Outdoor
μg m^{-3}												
WSOC	4.80	3.32	5.00	4.66	2.23	0.73	1.77	2.94	1.91	0.33	0.71	1.08
	3.2–6.4	1.11–5.54	3.25–7.33	ND-10.5	1.62–2.83	0.08–1.37	0.36–3.18	2.1–3.78	1.83–2	0.18–0.49	0.43–0.91	0.12–1.8
ng m^{-3}												
S	459	581	561	513	540	693	603	371	944	798	464	624
	390–528	554–608	416–901	297–760	436–644	597–790	481–726	65.1–677	780–1107	532–1063	343–618	416–890
Cl	170	491	220	617	129	130	105	38.9	451	597	73.5	249
	159–181	318–664	ND-390	107–1290	80.7–176	ND-259	45.2–166	25.1–52.8	267–635	155–1039	21.0–110	173–368
Ca	236	119	873	527	282	274	342	111	679	395	735	312
	195–278	91.5–146	628–1129	192–1166	237–326	192–357	266–417	31.5–190	656–701	197–593	58.8–2084	174–493
Ti	ND	ND	ND	63.3	59.4	ND	ND	28.6	70.5	53.9	26.5	10.3
				ND-253	ND-119			ND-57.2	ND-141	ND-108	ND-79.6	ND-17.5
V	8.27	13.8	7.50	6.79	ND	6.89	16.5	ND	14.9	9.40	4.21	3.77
	ND-16.5	ND-27.5	ND-30.0	ND-27.2		ND-13.8	ND-32.9		ND-29.8	ND-18.8	1.68–8.67	2.62–5.74
Cr	9.51	ND	3.98	1.62	ND	ND	ND	9.05	9.99	2.59	0.49	0.48
	ND-19.0		ND-15.4	ND-6.50				0.32–17.8	ND-19.9	ND-5.17	ND-1.46	ND-0.96
Mn	14.09	26.0	47.9	15.0	11.4	ND	46.5	38.7	ND	16.2	3.41	7.71
	ND-28.2	24.7–27.2	ND-81.2	ND-60.0	ND-22.8		36.1–56.8	32.8–44.6		ND-32.5	2.33–5.13	4.6–11.3
Fe	48.2	66.2	99.5	153	40.2	121	58.9	89.6	169	112	48.8	121
	18.5–78.0	10.1–122	68.2–172	63.7–295	29.1–51.3	106–135	55.2–62.6	79.4–99.9	162–176	60.7–164	37.9–54.7	68.0–209
Ni	4.88	ND	ND	ND	ND	4.25	12.1	5.77	ND	8.80	0.36	ND
	ND-9.75					ND-8.49	ND-24.1	ND-11.5		ND-17.6	ND-1.09	
Cu	ND	20.7	ND	ND	34.8	ND	52.6	ND	ND	ND	0.11	1.75
		ND-41.4			ND-69.7		ND-105				ND-0.34	ND-5.26
Zn	28.5	26.6	62.9	5.85	62.9	35.1	ND	ND	68.9	ND	8.85	30.9
	ND-57.0	ND-53.3	43.0–83.1	ND-18.5	36.3–89.4	ND-70.2			60.8–76.9		ND-15.1	9.19–54.5
Se	ND	ND	79.3	ND	104	ND	ND	34.6	ND	ND	ND	ND
			ND-133		81.2–126			ND-69.3				
As	52	ND	ND	33.4	90.8	ND	ND	ND	ND	ND	ND	ND
	ND-104			ND-134	81.6–100							
Sr	ND	ND	ND	ND	ND	ND	ND	ND	ND	ND	ND	2.15
												ND-6.45
Pb	ND	58.4	ND	ND	ND	57.8	ND	ND	ND	ND	ND	ND
		ND-117				ND-116						
Br	86.4	ND	80131	97.4	36202	24.8	50274	10.7	462	16.2	14.2	9.97
	74.2–98.7		48275–111599	3.09–193	25960–46443	ND-49.7	30785–69764	ND-21.5	273–651	ND-32.4	9.80–17.4	6.63–12.0
SO_4^{2-}	640	971	1004	1289	1072	1571	1742	3086	1583	1987	925	1645
	574–705	864–1078	620–1215	822–1733	868–1275	1265–1878	1434–2050	2842–3329	1416–1751	1670–2304	839–1069	1226–1955
NO_2^-	ND	18.9	ND	67.2	ND	ND	ND	18.6	ND	ND	ND	ND
		ND-37.9		ND-269				ND-37.1				
PO_4^{3-}	831	178	ND	ND	ND	ND	ND	172	328	ND	33.7	17.0
	ND-1663	ND-356						ND-344	ND-656		ND-60.9	ND-51.0
NO_3^-	3074	879	5362	1814	4248	1082	4359	2035	3929	1456	208	1449
	2567–3580	238–1519	503–9984	ND-4541	4043–4453	495–1669	3361–5357	1343–2727	3802–4056	1131–1781	153–271	1131–1786
F^-	ND	ND	ND	ND	ND	ND	ND	ND	ND	ND	62.1	80.3
											58.1–66.3	67.3–97.4
Li^+	15.4	ND	ND	ND	ND	ND	ND	ND	10.9	ND	ND	ND
	14.7–16.0								ND-21.7			
Na^+	ND	1456	1822	2481	ND	30.0	ND	895	ND	761	234	864
		232–2680	ND-4295	1009–3796		ND-60.0		742–1048		ND-1521	28.2–434	504–1422
K^+	370	166	1045	525.4	161	250.8	342	457	375	409	100	102
	297–443	151–180	926–1143	ND-958	152–171	219–283	314–370	367–547	375–376	231–586	41.4–172	100–105
Mg^{2+}	128	177	20.3	132	112	143	ND	40.6	124	207	24.4	107
	125–130	139–214	ND-43.0	29.6–204	92.6–130	88.5–198		37.4–43.8	62.6–184	176–238	7.19–47.9	57.6–193
NH_4^+	601	ND	14754	40.0	6790	424	11589	811	681	134	146	444
	533–668		11901–18346	ND-160	5374–8206	388–460	8473–14704	680–943	509–852	46.6–221	85.8–249	303–663

ND: not detected.

200 mL using the same burner type, WSOC concentrations decreased, although they remained considerably above background levels. For the same initial fuel load, the SC burner produced slightly higher WSOC concentrations than the DC when burning Fuel 1. Outdoors, WSOC concentrations were highly variable.

The elemental composition of PM_{10} revealed substantial changes during fireplace operation compared with background conditions (Table 5). Indoor levels varied markedly among elements and combustion configurations, indicating that emissions are strongly influenced by both fuel and burner design.

Sulphur, chlorine, calcium, potassium, and bromine dominated the elemental profile. Sulphur concentrations ranged from 459 to 944 ng m^{-3}, with higher values observed during Fuel 2 combustion. Chlorine also increased during combustion, with indoor levels up to 451 ng m^{-3} (Fuel 2, SC). Nevertheless, Fuel 2 DC was the only condition for which an I/O > 1 was observed. Sulphur and chlorine were below the detection limit in the fuels and in the ceramic wool (Table 1; Table S1). Calcium was consistently enriched indoors across all tests, especially for Fuel 1 DC* (873 ng m^{-3}), showing I/O > 1 for every combustion condition. Calcium was detected in both fuels and in the ceramic wool, suggesting that both fuel composition and burner materials may contribute to the observed indoor levels. Bromine displayed the most pronounced enrichment, with very high indoor concentrations for both fuels, particularly with DC burners (up to 80 μg m^{-3} for Fuel 1, DC*). The I/O ratios several orders of magnitude above unity indicate a dominant indoor source associated with combustion. Although bromine was below the detection limit in the fuels (Table 1), it was identified in the ceramic wool (Table S1), suggesting that burner materials may represent a source. Bromine is often associated with the emission of organobromine compounds or halogenated by-products of incomplete combustion [60]. These species may undergo redox reactions or form secondary oxidants (e.g., HOBr, BrO radicals), potentially enhancing oxidative stress through the generation of secondary aerosol enriched in oxidising functional groups.

Vanadium, chromium, manganese, iron, nickel, copper, and zinc were detected with variable patterns. Vanadium and chromium showed I/O > 1 for several tests, reaching 16.5 ng m^{-3} (Fuel 2, DC) and 9.99 ng m^{-3} (Fuel 2, SC), respectively. Manganese was strongly enhanced indoors, peaking at 47.9 ng m^{-3} (Fuel 1, DC*), while iron reached 169 ng m^{-3} (Fuel 2, SC) and exceeded outdoor levels only under this condition. Nickel was undetected in several combustion configurations; the highest concentration occurred during Fuel 2 combustion with the DC burner (12.1 ng m^{-3}). Copper was not detected in most experiments, reaching a maximum average concentration of 52.6 ng m^{-3} (Fuel 2, DC). Zinc was consistently higher indoors than outdoors in most configurations, with a maximum average concentration of 68.9 ng m^{-3} (Fuel 2, SC). Vanadium, chromium, manganese, nickel, copper, iron, and zinc were detected in both fuels (Table 1) and the ceramic wool (Table S1), indicating that emissions may originate from both fuel and burner materials. Furthermore, some of these elements may be released from the alloys of the combustion appliance when exposed to high temperatures [61]. Chromium may also originate from chromated copper arsenate, a preservative used in treated wood products such as furniture and building materials [62].

Arsenic and selenium were detected only during fireplace operation with Fuel 1, reaching indoor average concentrations of 90.8 ng m^{-3} and 104 ng m^{-3}, respectively, while outdoor levels remained below the detection limit. For comparison, the European Union Directive 2004/107/EC establishes an annual limit value of 6 ng m^{-3} for arsenic to protect human health. Arsenic and selenium in the fuels were below the detection limit. However, both elements were detected in the ceramic wool. Although this suggests that the burner filling is the potential source, their detection exclusively during Fuel 1 combustion indicates that release mechanisms might be influenced by other combustion-related parameters (e.g., temperature). Lead and strontium were not detected under any condition.

No consistent trend was observed regarding the effect of burner design. However, for some species (e.g. Br, Cu), the DC burner produced higher indoor concentrations than the SC burner. This suggests that the influence of burner geometry is element-specific, possibly reflecting variations in local temperature gradients and surface interactions within each design. No consistent relationship was observed between fuel type and indoor elemental concentrations, except in the case of arsenic and selenium.

The ionic composition of PM_{10} varied substantially between combustion and background conditions (Table 5). Indoor nitrate concentrations ranged from 3.1 to 5.4 μg m^{-3}, representing an enrichment of more than one order of magnitude compared with background (0.21 μg m^{-3}). Ammonium (NH_4^+) exhibited a behaviour similar to that of nitrate (NO_3^-) and was, in some cases, the most abundant species detected indoors (0.60 – 14.8 μg m^{-3}). In contrast, sodium (Na^+), potassium (K^+), magnesium (Mg^{2+}), and sulphate (SO_4^{2-}) concentrations were often higher outdoors.

Among all tested conditions, the DC* burner operating with Fuel 1 at the higher fuel load (250 mL) produced the highest indoor ionic concentrations, particularly for NH_4^+ (14.8 μg m^{-3}) and NO_3^- (5.4 μg m^{-3}). Both fuel composition and burner design influenced ion levels, although burner design exerted the strongest control on the largest variations. Compared with the SC burner, the DC led to substantially higher NH_4^+ concentrations (11.3 times higher for Fuel 1 and 17.0 times higher for Fuel 2) while NO_3^- exhibited more moderate increases (1.4 times higher for Fuel 1 and 1.1 times higher for Fuel 2). As previously mentioned, nitrogen oxides (NO and NO_2) produced in the flame are oxidised to nitric acid (HNO_3), which can subsequently react potentially leading to the formation of ammonium nitrate. This process likely occurs via gas-to-particle conversion during and shortly after combustion.

Differences between fuels were comparatively small. Fuel 2 tended to yield slightly higher NH_4^+ and NO_3^- concentrations than Fuel 1 under equivalent burner conditions. For the main combustion-related ions (NH_4^+ and NO_3^-), indoor concentrations consistently exceeded outdoor levels in all combustion tests, confirming their predominant indoor origin.

3.3. PM_{10} oxidative potential

Fig. 4 presents the volume-normalised oxidative potential (OP_V) for OP^{AA} and OP^{DTT} across different fuel-burner combinations and sampling environments. Average indoor OP^{AA} levels during fireplace operation ranged from 1.11 nmol min^{-1} m^{-3} (Fuel 2, DC) to 6.11 nmol min^{-1} m^{-3} (Fuel 1, DC*). In contrast, background OP^{AA} values were substantially lower (0.15 ± 0.04 nmol min^{-1} m^{-3}). Operation of the bioethanol fireplace increased OP^{AA} by approximately 7- to 40-fold relative to background concentrations. For most tested conditions, indoor OP^{AA} levels exceeded outdoor values, with two exceptions: combustion of Fuel 1 using the SC burner, where outdoor levels were higher, and combustion of Fuel 2 with the DC burner, where indoor and outdoor values were comparable.

OP^{DTT} exhibited a similar trend across indoor fuel-burner combinations. The highest OP^{DTT} value was observed for the DC burner operating with Fuel 1 at the highest fuel load (250 mL, 3.82 nmol min^{-1} m^{-3}), while the lowest occurred for Fuel 2 combustion using the DC burner (1.09 nmol min^{-1} m^{-3}). As with OP^{AA}, background indoor OP^{DTT} levels were considerably lower (0.18 ± 0.07 nmol min^{-1} m^{-3}). Operation of the bioethanol fireplace resulted in approximately 6- to 20-fold increase in OP^{DTT} relative to background levels. When comparing indoor and outdoor OP^{DTT} values, combustion of both fuels in the DC burner yielded higher indoor oxidative potential, whereas for the SC burner, outdoor OP^{DTT} values were slightly higher.

The substantial increases observed for both OP^{AA} and OP^{DTT} relative to background concentrations indicate a marked enhancement in the oxidative capacity of indoor PM during bioethanol fireplace operation. Previous studies have shown that OP^{AA} is more frequently associated

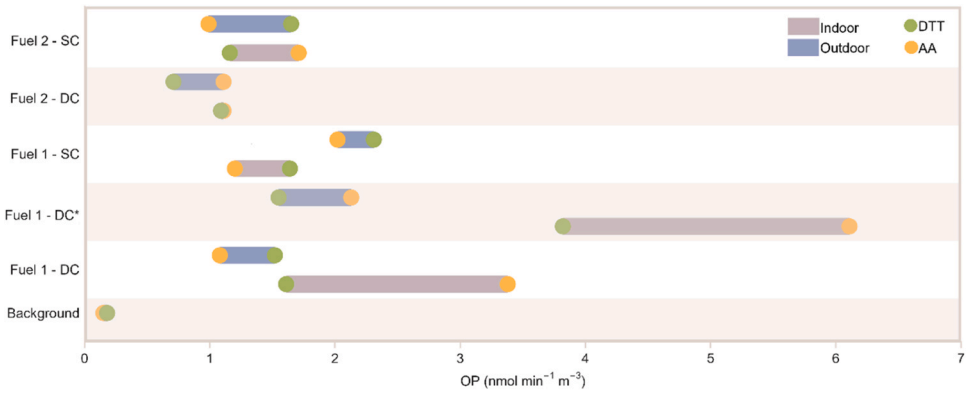

Fig. 4. Average OP_V levels indoors, during combustion and without indoor activities (background), and outdoors.

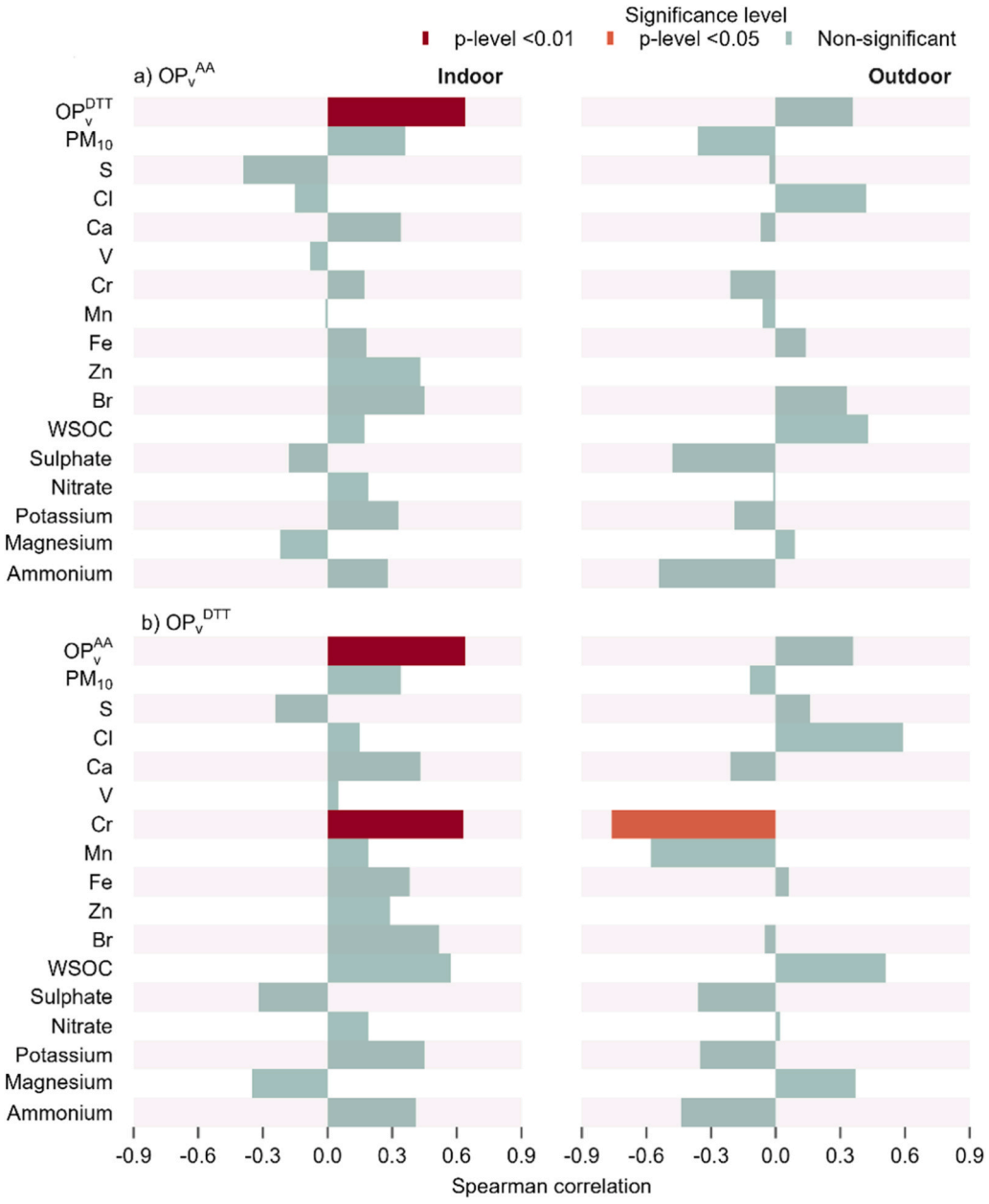

Fig. 5. Spearman correlations between chemical species concentrations and volume-normalised OP measured by two acellular assays (AA and DTT) in PM_{10} samples. The colour of the bars represents the significance of the correlations (p-values).

with biomarkers of oxidative stress and inflammation, whereas OP^{DTT} has demonstrated broader associations with cardiorespiratory and systemic health endpoints, albeit in an assay- and context-dependent manner [37,39]. The increase of both metrics therefore suggests that particles arising from bioethanol combustion may be relevant to multiple oxidative stress-related biological pathways.

The intrinsic oxidative potential (OP_m; pmol min^{-1} μg^{-1}) exhibited patterns distinct from those observed for the volume-normalised values (OP_V) (Table S2). OP^{AA} ranged from 6.89 to 46.3 pmol min^{-1} μg^{-1}, while OP^{DTT} varied between 6.70 and 86.5 pmol min^{-1} μg^{-1}. For both assays, the highest OP_m was recorded during the combustion of Fuel 1 using the SC burner, whereas the lowest OP_m occurred for Fuel 2 with the DC burner. The background OP_m values were generally lower than those measured under combustion conditions, with the exception of Fuel 2 in the DC burner, for which the OP_m values were comparable to or slightly lower than the background for both AA and DTT, and Fuel 1 DC for DTT. Outdoor OP_m levels showed substantial variability, ranging from 21.8 to 124 pmol min^{-1} μg^{-1} for the AA assay and 14.3–119 pmol min^{-1} μg^{-1} for the DTT assay.

Despite the growing use of bioethanol fireplaces and stoves, data on the OP of particles emitted from such systems is lacking. Existing studies have mainly examined OP associated with urban, traffic-related, or biomass-derived aerosols, leaving a clear gap regarding ethanol and bioethanol combustion in residential heating.

Although direct comparisons with other bioethanol combustion studies are not possible due to the lack of data, the mass-normalised OP values measured in the present study can be contextualised by comparison with emissions from conventional combustion appliances. Under some tested conditions, OP_m^{DTT} values were remarkably high (Table S1) relative to those reported for traditional stoves. For example, Zhan et al. [63] reported average OP_m^{DTT} values of 16 ± 7 pmol min^{-1} μg^{-1} for raw biomass, 7.6 ± 4.1 pmol min^{-1} μg^{-1} for biomass pellets, and 9.6 ± 4.2 pmol min^{-1} μg^{-1} for coal. Vicente et al. [64] evaluated the OP of indoor PM collected during the operation of solid fuel appliances (open fireplace, woodstove and coal stove) and reported OP_m^{DTT} average values ranging from 27 to 55 pmol min^{-1} μg^{-1}. The OP_m^{DTT} values observed in the present study are within the range reported for pellet stove emissions by Yang et al. [65]. That study investigated several indoor activities - including heating with a pellet stove, cooking on an electric stovetop, and burning incense - and found that pellet stove use resulted in the highest OP_m^{DTT} (55.9 ± 13.5 pmol min^{-1} μg^{-1}) compared with background (19.2 ± 16.5 pmol min^{-1} μg^{-1}). It should be noted, however, that the methodological approach differed, as Yang et al. [65] considered the total OP of $PM_{2.5}$ (soluble + insoluble fractions), whereas the present study focuses on the water-soluble fraction.

Spearman correlation coefficients between OPv and PM_{10} are presented in Fig. 5. A significant correlation between OP^{DTT} and OP^{AA} was observed indoors ($r = 0.636$, $p < 0.05$), whereas no significant relationship was found outdoors ($r = 0.364$, $p > 0.05$). Regarding the association between OP_V and PM_{10} concentrations, no significant correlations were detected in either environment. Indoors, a significant positive correlation was found between OP^{DTT} and Cr ($r = 0.632$, $p < 0.05$), while outdoors, the correlation was negative ($r = -0.758$, $p < 0.01$). The inverse association observed outdoors is consistent with previous findings by Ma et al. [66], who attributed this behaviour to complexation between Cr and humic-like substances (HULIS) in ambient particles. HULIS are abundant in outdoor PM, especially in areas influenced by biomass burning and SOA formation and are known contributors to DTT activity due to their redox-active functional groups. However, when Cr forms complexes with HULIS fractions (e.g, carboxyl and phenolic hydroxyl groups), these reactive sites become less available for electron transfer with DTT, thereby reducing the overall oxidative capacity of the aerosol [66]. In contrast, for the indoor environment, the positive correlation suggests that Cr may exist predominantly in more soluble or catalytically active forms, directly participating in electron transfer reactions with DTT. This difference highlights the potential influence of chemical speciation and local sources on the redox behaviour of Cr and its contribution to the OP of indoor versus outdoor PM. Beyond the correlations discussed above, no additional statistically significant associations were observed. The relatively small sample size may have further limited statistical power to detect relationships. In addition, variations in source composition or particle aging can modulate the influence of these species on the oxidative behaviour of the soluble fraction of ambient PM. Additionally, it is important to consider that in some studies, strong correlations between metals and particle oxidative activity may arise from the co-emission of metals with other redox-active species, rather than reflecting a direct or intrinsic relationship [67–70].

The correlations between OP_m (intrinsic OP) and the mass fractions of individual chemical species were analysed to assess how differences in PM chemical composition influence OP variability. The corresponding correlation coefficients are presented in Fig. 6. Compared with the OP_V, the OP_m exhibited distinct associations with PM constituents. Indoors, significant correlations of intrinsic OP^{DTT} were observed with Ca ($r = 0.609$, $p < 0.05$), Cr ($r = 0.863$, $p < 0.01$), WSOC ($r = 0.655$, $p < 0.01$), and K^+ ($r = 0.736$, $p < 0.01$), whereas OP^{AA} showed a significant correlation only with Cr ($r = 0.621$, $p < 0.05$). Outdoors, OP^{DTT} correlated significantly with Cl ($r = 0.718$, $p < 0.05$), S ($r = 0.727$, $p < 0.05$), and Mg^{2+} ($r = 0.764$, $p < 0.01$), while OP^{AA} also displayed significant positive correlations with Cl ($r = 0.736$, $p < 0.01$) and Mg^{2+} ($r = 0.636$, $p < 0.05$). The significant correlation of intrinsic OP^{DTT} with Ca indoors point to contributions from mineral/crustal dust. Mineral dust has measurable DTT activity and can elevate PM oxidative potential via co-emitted redox-active transition metals (e.g., Fe, Mn) [71,72]. In fact, in the present study significant correlations were observed between Ca and Mn and Fe (Figure S2). OP^{DTT} also showed a strong correlation with WSOC, reinforcing the role of carbonaceous components, particularly water-soluble organic compounds, in driving particulate OP [37,43,63,73–76]. Additionally, the significant correlations between OP^{DTT} and OP^{AA} and Cr further support the role of transition metals as key redox-active components driving DTT activity [77].

Outdoors, the observed relationships of intrinsic OP^{DTT} and OP^{AA} with Cl^-, and Mg^{2+} suggest the influence of mixed sources, including marine aerosols, and combustion emissions. In particular, Mg^{2+} and Cl^-, well-established tracers of sea-salt particles [78,79], indicate the contribution of marine air masses, and were significantly correlated in the outdoor samples. The absence of a correlation between intrinsic OP^{DTT} and WSOC suggests that using bulk carbonaceous fractions as surrogates for redox-active organics may obscure the variability among individual compounds with distinct oxidative properties [70].

3.4. Limitations

This study was designed to characterise the impact of a bioethanol fireplace on indoor air quality under controlled yet realistic operating conditions. Nonetheless, several limitations should be considered when interpreting the results.

All experiments were conducted under minimum ventilation conditions, with doors and windows closed. This approach was intentionally adopted to represent a conservative, worst-case exposure scenario, consistent with typical wintertime use. Consequently, the concentrations reported here reflect upper-bound indoor levels and are expected to vary under different ventilation conditions.

Only one fireplace model equipped with three burners was investigated. Although two burner designs and two commercial bioethanol fuels were evaluated, the variability associated with different fireplace brands, burner geometries, construction materials, and nominal heat output was not addressed. Consequently, the findings are representative of the tested configuration and should not be assumed to reflect the full range of bioethanol fireplaces available on the market.

For safety reasons, two occupants were present in the room during the combustion experiments, which may have influenced the measured

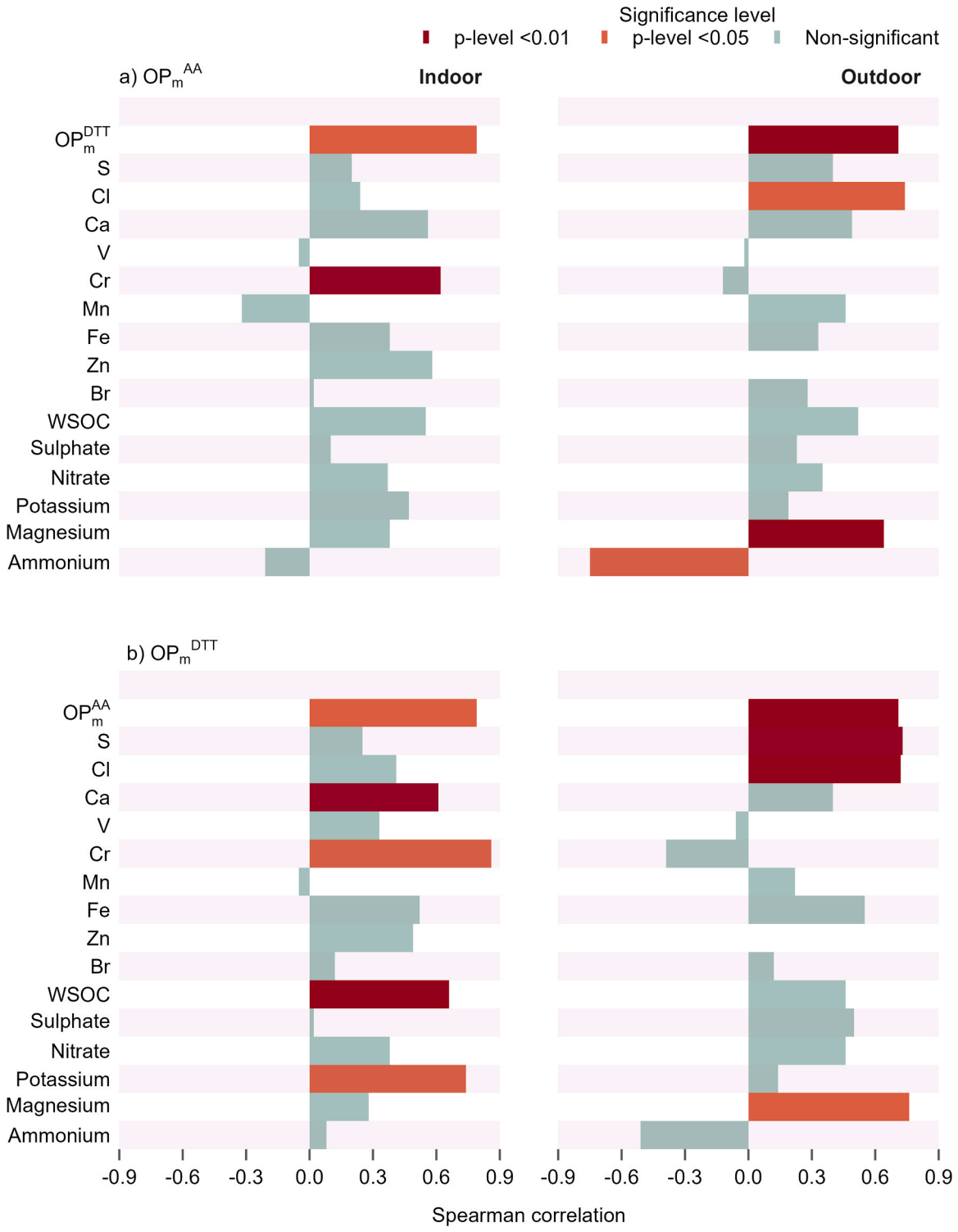

Fig. 6. Spearman correlations between chemical species mass fractions and mass-normalised OP measured by two acellular assays in PM_{10} samples.

pollutant levels. For example, human respiration contributed to indoor CO_2 concentrations, while occupant movement could have promoted particle resuspension. While background measurements without occupants were performed, the contribution of human presence to pollutant concentrations during combustion was not quantified and should be considered when interpreting the results.

Future research should build upon this work by evaluating different ventilation strategies, and a broader range of fireplace designs and fuel types.

4. Conclusions

This study provides a comprehensive evaluation of IAQ during the operation of a decorative bioethanol fireplace, focusing on the influence of burner design, fuel type, and fuel load. The results clearly demonstrate that, despite their perception as clean-burning devices, bioethanol fireplaces can significantly increase indoor concentrations of gaseous and particulate pollutants under typical use conditions.

Combustion led to marked increases in CO, CO_2, NO, NO_2, NH_3, N_2O,

C_2H_6O, and total VOCs, as well as in formaldehyde and acetaldehyde. Indoor concentrations of formaldehyde and NO_2 during combustion often surpassed the WHO short-term exposure guidelines. PM levels during fireplace operation also often surpassed recommended air quality limits, with PM_{10} reaching values up to 170 μg m^{-3}. The DC burner consistently produced higher indoor levels of CO, TVOCs, C_2H_6O, formaldehyde, acetaldehyde, PM_{10} and PM-bound compounds (Br, NH_4^+ and NO_3^-) whereas the SC burner was associated with greater NO indoor concentrations. For the other gaseous species, small differences were found between burner designs. Fuel composition also played a key role on indoor pollutant levels. Fuel 1 led to greater indoor concentrations of CO, formaldehyde and acetaldehyde compared to Fuel 2. PM_{10}, TVOCs and NO indoor concentrations were higher when Fuel 2 was burned. The influence of fuel load on emission behaviour was consistent across most pollutants. Increasing the amount of fuel burned (from 200 mL to 250 mL, Fuel 1, DC burner) generally led to higher pollutant concentrations, particularly for NO, NO_2, N_2O, PM_{10}, and PM_{10}-bound compounds (WSOC, Br, NH_4^+ and NO_3^-). An exception was observed for carbonyl compounds (formaldehyde and acetaldehyde), TVOCs, C_2H_6O, and CO, whose concentrations were slightly lower at higher fuel loads. Bioethanol fireplace operation markedly increased PM_{10} oxidative potential compared to background air. Indoor OP_V generally exceeded outdoor values, particularly for the DC burner operated with higher fuel load, though exceptions occurred depending on fuel and burner type. Correlations indicate that transition metals (especially Cr), mineral dust (Ca), and water-soluble organics (WSOC) drive indoor oxidative activity.

The findings indicate that even short-term use of flueless ethanol fireplaces can substantially degrade IAQ, especially in poorly ventilated environments. Compared with indoor concentrations reported during the operation of traditional wood-burning appliances, bioethanol combustion was associated with particularly elevated emissions of nitrogen oxides and aldehydes (formaldehyde and acetaldehyde), highlighting a distinct indoor pollution profile for this type of heating device. Based on the experimental results, to minimise indoor pollutant exposure, the use of higher-purity bioethanol fuels (low water content) is recommended, and full fuel loads should be avoided. Continuous or periodic ventilation during operation is strongly advised, together with additional ventilation immediately after flame extinction. Repeated or prolonged operations without ventilation should be avoided, particularly in small or poorly ventilated rooms.

Environmental implication

This study shows that bioethanol fireplaces, often marketed as clean, can significantly impair indoor air quality. Combustion led to marked increases in NO_2, NO, VOCs, PM_{10}, and carbonyl compounds, including formaldehyde and acetaldehyde, with some pollutants frequently exceeding health-based limits. PM_{10} also exhibited elevated oxidative potential, in some cases rising more than one order of magnitude above background levels. Emission profiles were strongly affected by burner design, fuel formulation, and fuel load. These results indicate that flueless bioethanol fireplaces may contribute substantially to indoor pollutant exposure and should inform future air quality regulations and consumer safety guidance.

CRediT authorship contribution statement

Célia Alves: Writing – review & editing, Resources, Project administration, Funding acquisition. **Jiří Ryšavý:** Writing – review & editing, Resources, Project administration, Methodology, Funding acquisition, Conceptualization. **Nuria Galindo:** Writing – review & editing, Resources, Project administration, Methodology, Investigation, Funding acquisition. **Eduardo Yubero:** Writing – review & editing, Resources, Investigation. **Mário Cerqueira:** Writing – review & editing, Resources, Methodology. **Manuel Feliciano:** Writing – review & editing, Resources. **Isabella Charres:** Visualization, Methodology, Investigation. **Teresa Nunes:** Writing – review & editing, Methodology. **Estela Domingos Vicente:** Writing – original draft, Visualization, Methodology, Investigation, Formal analysis, Conceptualization. **Yago Cipoli:** Visualization, Methodology, Investigation.

Declaration of Competing Interest

The authors declare that they have no known competing financial interests or personal relationships that could have appeared to influence the work reported in this paper.

Acknowledgments

Estela Vicente acknowledges the research contract under Scientific Employment Stimulus (DOI:10.54499/2022.00399.CEECIND/CP1720/CT0012) from the FCT - Fundação para a Ciência e a Tecnologia I.P. FCT is also acknowledged for the PhD scholarships to Y. Cipoli (SFRH/BD/04992/2021) and I. Charres (DOI:10.54499/2022.12142.BD). This work was supported by national funds through FCT, under the project/grant UID/50006 + LA/P/0094/2020 (doi.org/10.54499/LA/P/0094/2020), and through the project "Air Pollution in an African Megacity: Source Apportionment and Health Implications" (APAM, DOI: 10.54499/2022.04240.PTDC). Oxidative potential assays and the chemical characterisation of PM_{10} samples were partially funded by MCIN/AEI/10.13039/501100011033 and the "European Union NextGenerationEU/PRTR" (CAMBIO project, ref. TED2021–131336B-I00) and by MICIU/AEI/10.13039/501100011033 and ERDF/EU (TOXICAR project, ref. PID2023–149608OB-I00). This work was co-financed by the Technology Agency of the Czech Republic under the SIGMA DC2 Programme, project no. TQ03000511, "Innovative catalysts for household stationary heating units". The European Union also financially supported this work under the REFRESH—Research Excellence for Region Sustainability and High-tech Industries project No.CZ.10.03.01/00/22_003/0000048 via the Operational Programme Just Transition. European Union; MICIU (Spain Ministry of Science Innovation and Universities) /AEI (State Agency of Research); ERDF (European Regional Development Fund)/EU.

The authors would like to thank the Technical Management Services of the University of Aveiro for providing the necessary conditions to conduct the combustion experiments. Special thanks are extended to Technical Engineer Johnny Reis, Head of the Quality, Environment, and Safety Division at the University of Aveiro, for ensuring the required safety measures and providing essential logistical support.

Appendix A. Supporting information

Supplementary data associated with this article can be found in the online version at doi:10.1016/j.jhazmat.2026.141770.

Data availability

Data will be made available on request.

References

[1] HEI, State of Global Air 2024. Special Report, (2024) 1–35. ⟨https://www.stateofglobalair.org/sites/default/files/documents/2024-06/soga-2024-report_0.pdf⟩.
[2] Brasche, S., Bischof, W., 2005. Daily time spent indoors in German homes – Baseline data for the assessment of indoor exposure of German occupants. Int J Hyg Environ Health 208, 247–253. https://doi.org/10.1016/J.IJHEH.2005.03.003.
[3] Schweizer, C., Edwards, R.D., Bayer-Oglesby, L., Gauderman, W.J., Ilacqua, V., Juhani Jantunen, M., Lai, H.K., Nieuwenhuijsen, M., Künzli, N., 2007. Indoor time–microenvironment–activity patterns in seven regions of Europe. J Expo Sci Environ Epidemiol 17, 170–181. https://doi.org/10.1038/sj.jes.7500490.
[4] Nie, T., Zhang, G., Sun, Y., Wang, W., Wang, T., Duan, H., 2025. Effects of indoor air quality on human physiological impact: a review. Buildings 15, 1–21. https://doi.org/10.3390/buildings15081296.

[5] Mujan, I., Anđelković, A.S., Munćan, V., Kljajić, M., Ružić, D., 2019. Influence of indoor environmental quality on human health and productivity - A review. J Clean Prod 217, 646–657. https://doi.org/10.1016/j.jclepro.2019.01.307.

[6] Grassie, D., Milczewska, K., Renneboog, S., Scuderi, F., Dimitroulopoulou, S., 2025. Impact of indoor air quality, including thermal conditions, in educational buildings on health, wellbeing, and performance: a scoping review. Environments 12, 261. https://doi.org/10.3390/environments12080261.

[7] Y. Zhang, P.K. Hopke, C. Mandin, Handbook of Indoor Air Quality, 2022. https://doi.org/10.1007/978-981-16-7680-2.

[8] Singh, O.M., Devi, K.K., Khoiyangbam, R.S., 2025. The air within: reviewing the sources and health effects of indoor air pollution in households. Int J Environ Health Res 35, 1937–1957. https://doi.org/10.1080/09603123.2024.2415912.

[9] Carslaw, N., Bekö, G., Langer, S., Schoemaecker, C., Mihucz, V.G., Dudzinska, M., Wiesen, P., Nehr, S., Huttunen, K., Querol, X., Shaw, D., 2024. A new framework for indoor air chemistry measurements: Towards a better understanding of indoor air pollution. Indoor Environ 1, 100001. https://doi.org/10.1016/j.indenv.2023.100001.

[10] Goldstein, A.H., Nazaroff, W.W., Weschler, C.J., Williams, J., 2020. How do indoor environments affect air pollution exposure? Environ Sci Technol 55, 100–108. https://doi.org/10.1021/ACS.EST.0C05727.

[11] Farmer, D.K., Vance, M.E., Abbatt, J.P.D., Abeleira, A., Alves, M.R., Arata, C., Boedicker, E., Bourne, S., Cardoso-Saldaña, F., Corsi, R., Decarlo, P.F., Goldstein, A.H., Grassian, V.H., Hildebrandt Ruiz, L., Jimenez, J.L., Kahan, T.F., Katz, E.F., Mattila, J.M., Nazaroff, W.W., Novoselac, A., O'Brien, R.E., Or, V.W., Patel, S., Sankhyan, S., Stevens, P.S., Tian, Y., Wade, M., Wang, C., Zhou, S., Zhou, Y., 2019. Overview of HOMEChem: house observations of microbial and environmental chemistry. Environ Sci Process Impacts 21, 1280–1300. https://doi.org/10.1039/c9em00228f.

[12] Kumar, P., Singh, A.B., Arora, T., Singh, S., Singh, R., 2023. Critical review on emerging health effects associated with the indoor air quality and its sustainable management. Sci Total Environ 872, 162163. https://doi.org/10.1016/j.scitotenv.2023.162163.

[13] Yang, J., Duan, J., Niu, X., Hu, T., Huang, Y., Sun, J., Cao, J., 2025. A comprehensive review on indoor air pollutants and their health impacts: priority pollutants and suggested mitigations. Air Qual Atmos Heal 18, 2151–2184. https://doi.org/10.1007/s11869-025-01750-3.

[14] Sysoltseva, M., Winterhalter, R., Frank, A., Matzen, W., Fembacher, L., Scheu, C., Fromme, H., 2018. Physicochemical characterization of aerosol particles emitted by electrical appliances. Sci Total Environ 619–620, 1143–1152. https://doi.org/10.1016/J.SCITOTENV.2017.11.088.

[15] Patel, S., Sankhyan, S., Boedicker, E.K., Decarlo, P.F., Farmer, D.K., Goldstein, A.H., Katz, E.F., Nazaroff, W.W., Tian, Y., Vanhanen, J., Vance, M.E., 2020. Indoor particulate matter during HOMEChem: Concentrations, size distributions, and exposures. Environ Sci Technol 54, 7107–7116. https://doi.org/10.1021/acs.est.0c00740.

[16] Park, S., Song, D., Park, S., Choi, Y., 2021. Particulate matter generation in daily activities and removal effect by ventilation methods in residential building. Air Qual Atmos Heal 14, 1665–1680. https://doi.org/10.1007/s11869-021-01047-1.

[17] Ott, W.R., Zhao, T., Cheng, K.C., Wallace, L.A., Hildemann, L.M., 2021. Measuring indoor fine particle concentrations, emission rates, and decay rates from cannabis use in a residence. Atmos Environ X 10, 100106. https://doi.org/10.1016/J.AEAOA.2021.100106.

[18] O'Leary, C., de Kluizenaar, Y., Jacobs, P., Borsboom, W., Hall, I., Jones, B., 2019. Investigating measurements of fine particle ($PM_{2.5}$) emissions from the cooking of meals and mitigating exposure using a cooker hood. Indoor Air 29, 423–438. https://doi.org/10.1111/INA.12542.

[19] Stabile, L., Buonanno, G., Avino, P., Frattolillo, A., Guerriero, E., 2018. Indoor exposure to particles emitted by biomass-burning heating systems and evaluation of dose and lung cancer risk received by population. Environ Pollut 235, 65–73. https://doi.org/10.1016/j.envpol.2017.12.055.

[20] Embiale, A., Chandravanshi, B.S., Zewge, F., Sahle-Demessie, E., 2019. Investigation into trace elements in PM_{10} from the baking of Injera using clean, improved and traditional stoves: Emission and health risk assessment. Aerosol Sci Eng 34 (3), 150–163. https://doi.org/10.1007/S41810-019-00049-Y.

[21] Embiale, A., Zewge, F., Chandravanshi, B.S., Sahle-Demessie, E., 2019. Short-term exposure assessment to particulate matter and total volatile organic compounds in indoor air during cooking Ethiopian sauces (Wot) using electricity, kerosene and charcoal fuels. Indoor Built Environ 28, 1140–1154. https://doi.org/10.1177/1420326X19836453.

[22] Semmens, E.O., Noonan, C.W., Allen, R.W., Weiler, E.C., Ward, T.J., 2015. Indoor particulate matter in rural, wood stove heated homes. Environ Res 138, 93–100. https://doi.org/10.1016/j.envres.2015.02.005.

[23] Men, Y., Li, J., Liu, X., Li, Y., Jiang, K., Luo, Z., Xiong, R., Cheng, H., Tao, S., Shen, G., 2021. Contributions of internal emissions to peaks and incremental indoor $PM_{2.5}$ in rural coal use households. Environ Pollut 288, 117753. https://doi.org/10.1016/J.ENVPOL.2021.117753.

[24] Wang, D., Li, Q., Shen, G., Deng, J., Zhou, W., Hao, J., Jiang, J., 2020. Significant ultrafine particle emissions from residential solid fuel combustion. Sci Total Environ 715, 136992. https://doi.org/10.1016/J.SCITOTENV.2020.136992.

[25] Li, T., Cao, S., Fan, D., Zhang, Y., Wang, B., Zhao, X., Leaderer, B.P., Shen, G., Zhang, Y., Duan, X., 2016. Household concentrations and personal exposure of $PM_{2.5}$ among urban residents using different cooking fuels. Sci Total Environ 548–549, 6–12. https://doi.org/10.1016/j.scitotenv.2016.01.038.

[26] Vicente, E.D., Vicente, A.M., Evtyugina, M., Oduber, F.I., Amato, F., Querol, X., Alves, C., 2020. Impact of wood combustion on indoor air quality. Sci Total Environ 705, 135769. https://doi.org/10.1016/j.scitotenv.2019.135769.

[27] Vicente, E., Calvo, A.I., Sainnokhoi, T.A., Kováts, N., de la Campa, A.S., de la Rosa, J., Oduber, F., Nunes, T., Fraile, R., Tomé, M., Alves, C.A., 2024. Indoor PM from residential coal combustion: Levels, chemical composition, and toxicity. Sci Total Environ 918, 170598. https://doi.org/10.1016/j.scitotenv.2024.170598.

[28] European Commission, Study on alcohol-powered flueless fireplace combustion and its effects on indoor air quality, Brussels, 2015.

[29] Guillaume, E., Loferme-Pedespan, N., Duclerget-Baudequin, A., Raguideau, A., Fulton, R., Lieval, L., 2013. Ethanol fireplaces: safety matters. Saf Sci 57, 243–253. https://doi.org/10.1016/j.ssci.2013.03.003.

[30] Ryšavý, J., Vicente, E.A.D., Molchanov, O., Cipoli, Y.A., Krpec, K., Alves, C.A., Feliciano, M., Dargham, I., Kuo, J.K., Wang, C.C., 2025. Experimental study of thermo-environmental properties of single and double-chambered bioethanol burners. Appl Energy Combust Sci 23. https://doi.org/10.1016/j.jaecs.2025.100359.

[31] Martinka, J., Rantuch, P., Wachter, I., 2019. Impact of water content on energy potential and combustion characteristics of methanol and ethanol fuels. Energies 12. https://doi.org/10.3390/en12183491.

[32] Höllbacher, E., Ters, T., Rieder-Gradinger, C., Srebotnik, E., 2017. Emissions of indoor air pollutants from six user scenarios in a model room. Atmos Environ 150, 389–394. https://doi.org/10.1016/j.atmosenv.2016.11.033.

[33] Nozza, E., Capelli, L., Eusebio, L., Derudi, M., Nano, G., Del Rosso, R., Sironi, S., 2016. The role of bioethanol flueless fireplaces on indoor air quality: focus on odour emissions. Build Environ 98, 98–106. https://doi.org/10.1016/j.buildenv.2016.01.004.

[34] Schripp, T., Salthammer, T., Wientzek, S., Wensing, M., 2014. Chamber studies on nonvented decorative fireplaces using liquid or gelled ethanol fuel. Environ Sci Technol 48, 3583–3590. https://doi.org/10.1021/es404972s.

[35] Anderson, J.O., Thundiyil, J.G., Stolbach, A., 2012. Clearing the air: A review of the effects of particulate matter air pollution on human health. J Med Toxicol 8, 166–175. https://doi.org/10.1007/s13181-011-0203-1.

[36] Morawska, L., Afshari, A., Bae, G.N., Buonanno, G., Chao, C.Y.H., Hänninen, O., Hofmann, W., Isaxon, C., Jayaratne, E.R., Pasanen, P., Salthammer, T., Waring, M., Wierzbicka, A., 2013. Indoor aerosols: From personal exposure to risk assessment. Indoor Air 23, 462–487. https://doi.org/10.1111/ina.12044.

[37] Bates, J.T., Fang, T., Verma, V., Zeng, L., Weber, R.J., Tolbert, P.E., Abrams, J.Y., Sarnat, S.E., Klein, M., Mulholland, J.A., Russell, A.G., 2019. Review of acellular assays of ambient particulate matter oxidative potential: methods and relationships with composition, sources, and health effects. Environ Sci Technol 53, 4003–4019. https://doi.org/10.1021/acs.est.8b03430.

[38] Øvrevik, J., 2019. Oxidative potential versus biological effects: a review on the relevance of cell-free/abiotic assays as predictors of toxicity from airborne particulate matter. Int J Mol Sci 20. https://doi.org/10.3390/ijms20194772.

[39] Gao, D., Ripley, S., Weichenthal, S., Godri Pollitt, K.J., 2020. Ambient particulate matter oxidative potential: Chemical determinants, associated health effects, and strategies for risk management. Free Radic Biol Med 151, 7–25. https://doi.org/10.1016/j.freeradbiomed.2020.04.028.

[40] He, L., Zhang, J., 2023. Particulate matter (PM) oxidative potential: Measurement methods and links to PM physicochemical characteristics and health effects. Crit Rev Environ Sci Technol 53, 177–197. https://doi.org/10.1080/10643389.2022.2050148.

[41] Ryšavý, J., Horák, J., Kuboňová, L., Hopan, F., Krpec, K., Kubesa, P., Molchanov, O., Ochodek, T., 2020. Real operating parameters of bioethanol burners in terms of heat output. ACS Omega 5, 28587–28596. https://doi.org/10.1021/acsomega.0c03481.

[42] Vicente, E.D., Evtyugina, M., Vicente, A.M., Calvo, A.I., Oduber, F., Blanco-Alegre, C., Castro, A., Fraile, R., Nunes, T., Lucarelli, F., Calzolai, G., Alves, C.A., 2021. Impact of ironing on indoor particle levels and composition. Build Environ 192. https://doi.org/10.1016/j.buildenv.2021.107636.

[43] Gómez-Sánchez, N., Galindo, N., Alfosea-Simón, M., Nicolás, J.F., Crespo, J., Yubero, E., 2024. Chemical composition of PM_{10} at a rural site in the western Mediterranean and its relationship with the oxidative potential. Chemosphere 363. https://doi.org/10.1016/j.chemosphere.2024.142880.

[44] Chiari, M., Yubero, E., Calzolai, G., Lucarelli, F., Crespo, J., Galindo, N., Nicolás, J.F., Giannoni, M., Nava, S., 2018. Comparison of PIXE and XRF analysis of airborne particulate matter samples collected on Teflon and quartz fibre filters. Nucl Instrum Methods Phys Res Sect B Beam Interact Mater At 417, 128–132. https://doi.org/10.1016/j.nimb.2017.07.031.

[45] Salthammer, T., Schripp, T., Wientzek, S., Wensing, M., 2014. Impact of operating wood-burning fireplace ovens on indoor air quality. Chemosphere 103, 205–211. https://doi.org/10.1016/j.chemosphere.2013.11.067.

[46] Vicente, E.D., Vicente, A.M., Evtyugina, M., Oduber, F.I., Amato, F., Querol, X., Alves, C., 2020. Impact of wood combustion on indoor air quality. Sci Total Environ 705. https://doi.org/10.1016/j.scitotenv.2019.135769.

[47] Canha, N., Lage, J., Galinha, C., Coentro, S., Alves, C., Almeida, S.M., 2018. Impact of biomass home heating, cooking styles, and bread toasting on the indoor air quality at Portuguese dwellings: A case study. Atmosphere (Basel) 9. https://doi.org/10.3390/atmos9060214.

[48] Castro, A., Calvo, A.I., Blanco-Alegre, C., Oduber, F., Alves, C., Coz, E., Amato, F., Querol, X., Fraile, R., 2018. Impact of the wood combustion in an open fireplace on the air quality of a living room: Estimation of the respirable fraction. Sci Total Environ 628–629, 169–176. https://doi.org/10.1016/j.scitotenv.2018.02.001.

[49] Ryšavý, J., Horák, J., Krpec, K., Hopan, F., Kuboňová, L., Molchanov, O., 2022. Influence of fuel mixture and catalyst on the ethanol burner flue gas composition. Energy Rep 8, 871–879. https://doi.org/10.1016/j.egyr.2022.10.181.

[50] Saxena, P., Williams, F.A., 2007. Numerical and experimental studies of ethanol flames. Proc Combust Inst 31 (I), 1149–1156. https://doi.org/10.1016/j.proci.2006.08.097.
[51] Lévesque, B., Allaire, S., Gauvin, D., Koutrakis, P., Gingras, S., Rhainds, M., Prud'Homme, H., Duchesne, J.F., 2001. Wood-burning appliances and indoor air quality. Sci Total Environ 281, 47–62. https://doi.org/10.1016/S0048-9697(01)00834-8.
[52] Shrestha, K.P., Seidel, L., Zeuch, T., Mauss, F., 2018. Detailed kinetic mechanism for the oxidation of ammonia including the formation and reduction of nitrogen oxides. Energy Fuels 32, 10202–10217. https://doi.org/10.1021/acs.energyfuels.8b01056.
[53] Salthammer, T., 2022. Acetaldehyde in the indoor environment. Environ Sci Atmos 3, 474–493. https://doi.org/10.1039/d2ea00146b.
[54] Kohse-Höinghaus, K., Oßwald, P., Cool, T.A., Kasper, T., Hansen, N., Qi, F., Westbrook, C.K., Westmoreland, P.R., 2010. Biofuel combustion chemistry: from ethanol to biodiesel. Angew Chem Int Ed 49, 3572–3597. https://doi.org/10.1002/anie.200905335.
[55] de Gennaro, G., Dambruoso, P.R., Di Gilio, A., di Palma, V., Marzocca, A., Tutino, M., 2015. Discontinuous and continuous indoor air quality monitoring in homes with fireplaces or wood stoves as heating system. Int J Environ Res Public Health 13, 1–9. https://doi.org/10.3390/ijerph13010078.
[56] Cipoli, Y.A., Vicente, E.D., Charres, I., Evtyugina, M., Alfosea-Simón, M., Lucarelli, F., Kováts, N., Ryšavý, J., Feliciano, M., Alves, C., 2026. Comprehensive assessment of PM_{10} from home heating using different appliances and biomass fuels: Chemical composition, oxidative potential, and ecotoxicity. Atmos Environ 365. https://doi.org/10.1016/j.atmosenv.2025.121700.
[57] Webb, M., Morrison, G., Baumann, K., Li, J., Ditto, J.C., Huynh, H.N., Yu, J., Mayer, K., Mael, L., Vance, M.E., Farmer, D.K., Abbatt, J., Poppendieck, D., Turpin, B.J., 2024. Dynamics of residential indoor gas- and particle-phase water-soluble organic carbon: measurements during the CASA experiment. Environ Sci Process Impacts 27, 1535–1550. https://doi.org/10.1039/d4em00340c.
[58] Duarte, R.M.B.O., Duarte, A.C., 2021. On the water-soluble organic matter in inhalable air particles: Why should outdoor experience motivate indoor studies? Appl Sci 11. https://doi.org/10.3390/app11219917.
[59] Zhang, B., Xu, H., Gu, Y., Bai, Y., Wang, D., Yang, L., Sun, J., Shen, Z., Cao, J., 2024. Exploring the relationship between personal exposure to multiple water-soluble components and ROS in size-resolved PMs in solid fuel combustion households. Environ Pollut 363, 125075. https://doi.org/10.1016/j.envpol.2024.125075.
[60] Vainikka, P., Hupa, M., 2012. Review on bromine in solid fuels. Part 1: Natural occurrence. Fuel 95, 1–14. https://doi.org/10.1016/j.fuel.2011.11.068.
[61] Brady, M.P., Banta, K., Mizia, J., Lorenz, N., Leonard, D.N., Yamamoto, Y., DeFoort, M., Keiser, J.R., 2017. Alloy corrosion considerations in low-cost, clean biomass cookstoves for the developing world. Energy Sustain Dev 37, 20–32. https://doi.org/10.1016/j.esd.2016.12.002.
[62] Rivas, I., Viana, M., Moreno, T., Bouso, L., Pandolfi, M., Alvarez-Pedrerol, M., Forns, J., Alastuey, A., Sunyer, J., Querol, X., 2015. Outdoor infiltration and indoor contribution of UFP and BC, OC, secondary inorganic ions and metals in $PM_{2.5}$ in schools. Atmos Environ 106, 129–138. https://doi.org/10.1016/J.ATMOSENV.2015.01.055.
[63] Zhang, L., Li, Y., Li, J., Xing, R., Liu, X., Zhao, J., Shen, G., Pan, B., Li, X., Tao, S., 2024. Pollutant emissions and oxidative potentials of particles from the indoor burning of biomass pellets. Environ Sci Technol 58, 16016–16027. https://doi.org/10.1021/acs.est.4c03967.
[64] Vicente, E.D., Charres, I., Cipoli, Y., Calvo, A.I., Fraile, R., Candeias, C., Rocha, F., Galindo, N., Yubero, E., Alves, C., 2026. Indoor PM_{10} from fireplace, wood- and coal stove: morphology, composition, and oxidative potential in real residential settings. Environ Pollut 390. https://doi.org/10.1016/j.envpol.2025.127510.
[65] Yang, Y., Battaglia, M.A., Robinson, E.S., DeCarlo, P.F., Edwards, K.C., Fang, T., Kapur, S., Shiraiwa, M., Cesler-Maloney, M., Simpson, W.R., Campbell, J.R., Nenes, A., Mao, J., Weber, R.J., 2024. Indoor–outdoor oxidative potential of $PM_{2.5}$ in wintertime Fairbanks, Alaska: Impact of air infiltration and indoor activities. ACS ES&T Air 1, 188–199. https://doi.org/10.1021/acsestair.3c00067.
[66] Ma, X., Nie, D., Chen, M., Ge, P., Liu, Z., Ge, X., Li, Z., Gu, R., 2021. The relative contributions of different chemical components to the oxidative potential of ambient fine particles in Nanjing area. Int J Environ Res Public Health 18, 1–17. https://doi.org/10.3390/ijerph18062789.
[67] Yu, H., Puthussery, J.V., Wang, Y., Verma, V., 2021. Spatiotemporal variability in the oxidative potential of ambient fine particulate matter in the Midwestern United States. Atmos Chem Phys 21, 16363–16386. https://doi.org/10.5194/acp-21-16363-2021.
[68] Shahpoury, P., Zhang, Z.W., Arangio, A., Celo, V., Dabek-Zlotorzynska, E., Harner, T., Nenes, A., 2021. The influence of chemical composition, aerosol acidity, and metal dissolution on the oxidative potential of fine particulate matter and redox potential of the lung lining fluid. Environ Int 148, 106343. https://doi.org/10.1016/j.envint.2020.106343.
[69] Yu, H., Wang, Y., Puthussery, J.V., Verma, V., 2024. Sources of acellular oxidative potential of water-soluble fine ambient particulate matter in the midwestern United States. J Hazard Mater 474, 134763. https://doi.org/10.1016/j.jhazmat.2024.134763.
[70] Gao, D., Mulholland, J.A., Russell, A.G., Weber, R.J., 2020. Characterization of water-insoluble oxidative potential of $PM_{2.5}$ using the dithiothreitol assay. Atmos Environ 224, 117327. https://doi.org/10.1016/j.atmosenv.2020.117327.
[71] Li, J., Hua, C., Ma, L., Chen, K., Zheng, F., Chen, Q., Bao, X., Sun, J., Xie, R., Bianchi, F., Kerminen, V.M., Petäjä, T., Kulmala, M., Liu, Y., 2024. Key drivers of the oxidative potential of $PM_{2.5}$ in Beijing in the context of air quality improvement from 2018 to 2022. Environ Int 187. https://doi.org/10.1016/j.envint.2024.108724.
[72] Nishita-Hara, C., Kobayashi, H., Hara, K., Hayashi, M., 2023. Dithiothreitol-measured oxidative potential of reference materials of mineral dust: Implications for the toxicity of mineral dust aerosols in the atmosphere. GeoHealth 7. https://doi.org/10.1029/2022GH000736.
[73] Wang, Y., Plewa, M.J., Mukherjee, U.K., Verma, V., 2018. Assessing the cytotoxicity of ambient particulate matter (PM) using Chinese hamster ovary (CHO) cells and its relationship with the PM chemical composition and oxidative potential. Atmos Environ 179, 132–141. https://doi.org/10.1016/j.atmosenv.2018.02.025.
[74] Li, R., Yan, C., Tian, Y., Wu, Y., Zhou, R., Meng, Q., Fang, L., Yue, Y., Yang, Y., Chen, H., Yang, L., Jiang, W., 2025. Insights into relationship of oxidative potential of particles in the atmosphere and entering the human respiratory system with particle size, composition and source: A case study in a coastal area in Northern China. J Hazard Mater 485, 136842. https://doi.org/10.1016/j.jhazmat.2024.136842.
[75] Sharma, B., Mao, J., Jia, S., Sharma, S.K., Mandal, T.K., Bau, S., Sarkar, S., 2024. Size-distribution and driving factors of aerosol oxidative potential in rural kitchen microenvironments of northeastern India. Environ Pollut 343, 123246. https://doi.org/10.1016/j.envpol.2023.123246.
[76] Janssen, N.A.H., Yang, A., Strak, M., Steenhof, M., Hellack, B., Gerlofs-Nijland, M. E., Kuhlbusch, T., Kelly, F., Harrison, R., Brunekreef, B., Hoek, G., Cassee, F., 2014. Oxidative potential of particulate matter collected at sites with different source characteristics. Sci Total Environ 472, 572–581. https://doi.org/10.1016/j.scitotenv.2013.11.099.
[77] Visentin, M., Pagnoni, A., Sarti, E., Pietrogrande, M.C., 2016. Urban $PM_{2.5}$ oxidative potential: Importance of chemical species and comparison of two spectrophotometric cell-free assays. Environ Pollut 219, 72–79. https://doi.org/10.1016/j.envpol.2016.09.047.
[78] Chi, J.W., Li, W.J., Zhang, D.Z., Zhang, J.C., Lin, Y.T., Shen, X.J., Sun, J.Y., Chen, J. M., Zhang, X.Y., Zhang, Y.M., Wang, W.X., 2015. Sea salt aerosols as a reactive surface for inorganic and organic acidic gases in the Arctic troposphere. Atmos Chem Phys 15, 11341–11353. https://doi.org/10.5194/acp-15-11341-2015.
[79] Xiao, H.W., Xiao, H.Y., Shen, C.Y., Zhang, Z.Y., Long, A.M., 2018. Chemical composition and sources of marine aerosol over the western north Pacific ocean in winter. Atmosphere 9. https://doi.org/10.3390/atmos9080298.